Response to reviewer # 1

Based on CTD/XCTD obtained in May 2012 and Argo profiles along the Carlsberg Ridge, this study discussed water masses over the specific section, showed a ventilation structure, and calculated the absolute geostrophic currents. This study is interesting. However, I have the following concerns.

One of the main weaknesses is that this paper does not have a clear scientific theme and draws some quick conclusions. The authors first showed the observed temperature, salinity, and density. Then, they calculated the geostrophic currents and compared the results with SODA and HYCOM. Finally, they set some passive tracers at 100m and 700m and tried to reveal pathways of the masses. It is difficult for the readers to understand what the paper focused on, just like we cannot obtain enough information in science from the title "Hydrographic survey over the Carlsberg Ridge in May 2012" Because of no in-depth analysis, the paper looks like a data analysis report, and the conclusions are not very convinced.

I thus suggest the authors focus on the water masses in the NWIO. The authors may want to start their analysis based on the CTD/XCTD data. Then, the obtained conclusions are expected to be verified using more data (e.g. more Argo profiles) in this region and more conclusions are expected. Finally, the analysis in section 3.4 is expected to be more solid to reveal the pathway of the water masses. The authors may want to delete the contents in section 3.3.

Response: We agree with reviewer's comments and suggestions. We revised the manuscript by

(1) We added the background on meso-scale eddy and west-propagating disturbance (changed to "west-propagating planetary wave (WPPW)") in Introduction Section, like

"Besides, the planetary waves at-least include Rossby and Kelvin waves (Rhines, 1975; McCreary, 1985). Satellite-retrieved sea surface height are commonly used to detect the planetary waves (Chelton and Schlax, 1996), however, the internal dynamics of planetary wave is not sufficiently addressed. The phase speed of west-propagating planetary wave (WPPW) is used to match the theoretical Rossby wave, nonetheless, the vertical structure of WPPW calls for vertical profiling observation (Subrahmanyam et al., 2001)."

(2) We moved the background of Red Sea Water from Results Section into Introduction Section, as

"For instance, three water masses were defined in NWIO as Arabian Sea High-Salinity Water (ASHSW), Persian Gulf Water (PGW) and Red Sea Water (RSW). Regarding the pathways of these water masses, the mechanics are not clear. RSW is formed near the northern side of the NWIO; therefore, according to the customary ocean ventilation theory, RSW sinks and moves southward along the isopycnal layer from the generation zone following the wind-driven current (Luyten et al., 1983). However, the applicability of the ocean ventilation theory is still unknown for the northern IO, because the surface wind reverses direction under the influence of wind monsoon (Liu et al., 2018). Meanwhile, the limited meridional extent of IO omits the polar-to-subpolar front, which helps form intermediate water in Pacific Ocean and Atlantic Ocean (You, 1998). In contrast, in situ potential vorticity analysis on RSW reveals that the flows generally follow the zonal direction (Beal et al., 2000). How the water mass moves is worthy further investigation."

(3) We added discussions on the main results of Lagrangian tracers (Section 3.4).

Therefore the main results include the snapshot of water masses, and the vertical structures of mesoscale eddy and west-propagating planetary wave.

Some minor comments:

1. Could you add the latitude (or longitude) in the x-axis of Fig. 3?

Response: Corrected.

2. "Wind and SST have a close relationship." The wind pattern may be not a key factor for the SST distribution in the oceanic interior.

Response: We deleted the statement "Wind and SST have a close relationship".

Response to reviewer # 2

This manuscript introduces hydrographic observations collected over the Carlsberg Ridge in the northwest Indian Ocean. The authors have created a hydrographic dataset that comprises observations collected by a ship and by Argo floats. They identify key water masses, conduct particle tracking experiments, and use the observations to evaluate two re-analysis products. With a few exceptions, the standard of written English is acceptable and the quality of the figures is, on the whole, satisfactory. I think that this manuscript will require substantial revision prior to publication.
Response: We are thankful to review's encouragement and constructive suggestions. We made major revision on the early version manuscript.

Point 1. My primary criticism of this manuscript is that it lacks a clear message; I am unsure of what it is that the authors want me to remember as being important or new. The authors correctly point out that the northwest Indian Ocean is not well sampled, and so any new observations from this region are of value. However, beyond simply presenting these new observations, the authors, in my view, do not sufficiently demonstrate what we can learn from them. The discussion section, which is where the value of the new observations should be made explicit, largely restates points already made in the results section. It does not cite a single piece of literature. I think that the discussion section needs to be substantially revised: it should explain the value of the observations in the context of relevant literature and, ideally, it should set out a clear argument.
Response: The main motivation is to understand the ocean environment over Carlsberg Ridge (CR). The novelty lies on the extra information brought by in-situ CTD & XCTD data. The sectional snapshot therefore gives the vertical structures of temperature, salinity, density and geostrophic current. In the revised manuscript, we emphasized three valuable results: (1) The snapshot of water masses, (2) the structure of mesoscale eddy, and (3) the structure of west-propagating disturbance (changed to "west-propagating planetary wave"). We revised the Introduction and Discussion sections, accordingly.

Point 2. The methods outlined in section 2 need to be better explained. The authors note the depth-mean offsets between temperature and salinity observations collected by the ship's CTD and the expendable CTDs (xCTD), and between the xCTDs and an Argo float. Firstly, the implication is that these offsets used to calibrate the xCTD observations ? but this should be stated explicitly. Secondly, it is not clear to me whether: (1) xCTD observations are being compared to both ship and Argo observations; or (2) whether ship observations are being compared to xCTD observations, which are then being compared to Argo observations. If the former, which of the two sets of off- sets are the authors using for the calibration? If the latter, are the authors calibrating observations from all Argo floats using an offset calculated from just one Argo float? Furthermore, do publicly available observations from the Argo programme need to be calibrated? Are they already calibrated when they are made available for download?

Response: [Page 3, line 28–31 in change-track-mode revised manuscript] Thanks for the suggestions. We did not calibrate the instrumental readings. XCTD observations were compared to both ship CTD and Argo observation. However, every XCTD and Argo has individual sensor, we did not impose calibration on these datasets. In the revised manuscript, we stated as:
"Differences among CTD, XCTD and Argo are not negligible. However, because the distances between two stations in comparisons are relatively large, and the biases of XCTD and Argo are different for instruments, we does not perform instrument calibration."
In addition, Argo data are not need further calibrated, the official site already made data quality control.

Point 3. The authors point out several times that adding the Argo observations to the ship CTD and XCTD observations enables them to examine mesoscale processes. This may well be the case, but I think that they need to carefully consider the temporal and spatial scales of mesoscale activity in the Arabian Sea. For instance, they include Argo observations from up to 200 km from their section over the Carlsberg Ridge: is this distance less than the Rossby radius at this latitude? Furthermore, Table 1 indicates that the observations were collected over a period of one month. Are the authors confident that these observations may be presented in one section (Figure 4) as if they were a synoptic snapshot?
Response: In the monthly mean sea surface height (Fig. 2c in revised manuscript), two dynamics include meso-scale eddy and west-propagating planetary wave are identified, we therefore confirm the two dynamics are beyond the synoptic snapshot.

Line-by-line comments.
Page 1, line 14. I am not sure what the authors mean by "renewed" in this context.
Response: [Page 1, line 14 in change-track-mode revised manuscript] We deleted the "renewed".

Page 1, lines 15–17. I am not really sure what this sentence means.
Response: [Page 1, line 15-16, in change-track-mode revised manuscript]
"Moreover, the monsoon builds up a meridional current in the NWIO, which changing the form of the customary zonal current (as in the Pacific and Atlantic Oceans) into the meridional current."
was changed to
"Moreover, the monsoon is strong to change the pattern of basin-scale circulation. The monsoon builds up a dominant meridional current in the NWIO, changing the form of the customary zonal current (as in the Pacific and Atlantic Oceans) into a meridional current."

Page 1, paragraph beginning line 21. This paragraph is not relevant
Response: We deleted the paragraph.

Page 2, paragraph beginning line 13. This paragraph outlines the reasons for studying the hydrography of the Carlsberg Ridge region, but none of the points raised is revisited later in the paper. The paper would be much improved if, when discussing the results, the authors revisited some of these points for instance, saying how these new observations help to determine the movements of sporadic hydrothermal activity.

Response: [Page 2, line 32–35; and Page 14, line 18–25, in change-track-mode revised manuscript] We revised the motivation of present work at the end of Introduction:

"First, hydrographic survey takes a snapshot on the water mass, and gives an evidence on the activity of water mass. Second, the observation probably captures the vertical structure of meso-scale eddy or planetary wave. Third, the results could be used to evaluate the widely-used oceanic reanalysis. "

Furthermore, we added the discussion involving hydrothermal activity in Discussion Section, as

"Generally, the hydrothermal plume in CR uplifts from sea bottom to water depth 2500 m (Murton et al., 2006, Wang et al., 2017). Present paper restricts the sectional study to the upper 1050 m (Fig. 4-5). Within this depth, the water is easily affected by surface forcing. However, on the basin-scale wind-driven circulation, the surface wind forcing affects deeper ocean through quasi-geostrophic instability (Rhines and Young, 1982) and meridional overturning circulation. Because present paper concentrates on the CR as well as the cross-ridge current, the upper 1050 m dynamics towards the upper ocean cross-ridge water transport, which is related to the deeper ocean dynamics through pressure adjustment, meanwhile, the activity of meso-scale eddy induces deeper ocean vorticity response (Rhines and Young, 1982), the results provide potential use in the future study of hydrothermal plume event."

Page 2, line 17. I do not agree that the results presented "shed new light into the basic energy theory of ocean circulation"

Response: [Page 3, line 2, in change-track-mode revised manuscript] We deleted the statement..

Page 2, line 33. It would be nice to have the distance between the CTD and the xCTD station given in km.

Response: [Page 3, line 18, in change-track-mode revised manuscript] We added the distance in km

Page 3, line 6. Again, it would be nice to have the distance between the Argo and the xCTD station given in km.

Response: [Page 3, line 24, in change-track-mode revised manuscript] We added the distance in km

Page 4, Figure 1. I think that panel (a) is too small to be of much use: I can't really see the detail because the symbols are too close together. Panel (a) might work better as a separate figure. Similarly, I cannot distinguish individual vorticity contours in panel (b). Contours are not labelled, and the contour interval is not given. The vorticity field should be presented using filled contours, similar to the ADT field in panel (d).

Response: We revised the Figure 1 according to reviewer's suggestions.

Page 5, line 28. I assume that the data extracted from the re-analysis products are along the same section as the observations, but this should be said explicitly.

Response: [Page 6, line 19, in change-track-mode revised manuscript] Yes. We added a statement in section 2.4, as

"For comparison, we extract the reanalysis datasets along the same section as the observations, and the monthly mean fields are used."

Page 6, line 8 (equations). The symbol w is not defined. I assume it is vertical velocity? The authors should state whether they are performing their particle tracking experiments using 2D or 3D velocity.

Response: [Page 6, line 25-26, in change-track-mode revised manuscript] In section 2.5, we insert two sentences, as

"w is the vertical velocity"

and

"we use the three dimensional velocity (U, V, w) to track the tracers,"

Page 6, line 10. The authors give the start and end time of the particle tracking experiments here, and not in the caption of Figure 6.

Response:[Page 7, line 1–2, in change-track-mode revised manuscript] Corrected.

Page 6, line 19. I do not understand what the authors mean when they say that the "wind stress curl highlights the strong seasonal variations". Also, wind stress curl is not shown in a figure.

Response: [Page 7, line 12, in change-track-mode revised manuscript] We deleted the sentence.

Page 6, line 27. The statement that warm-core eddies "seem to release footprints in the wind stress curl" does not make sense. I would have thought that the wind influences the eddies and not the other way around. Furthermore, when talking about wind stress curl, the authors refer to Figure 1 (b), but the figure caption says that this panel shows wind velocity and vorticity, not wind stress curl.

Response: [Page 7, line 20–21, in change-track-mode revised manuscript] We deleted the sentence.

Page 6, 29. It is not clear why the westward current is "remarkable". Has this feature not been observed before? Is it significant? Do the authors believe that it cannot be explained by their observations, or by existing theory?

Response: [Page 7, line 12, in change-track-mode revised manuscript] We noted the westward current "remarkable" according to the magnitude and zonal extent. Present observation displays the vertical structure of this westward current (west propagating planetary wave, WPPW).

We added discussion on this west propagating planetary wave in Section Discussion, as

"From the theoretical viewpoint, the phase speed of first-, second- and third-mode baroclinic

Rossby wave at 6°N in Indian Ocean is roughly 0.6, 0.2 and 0.1 m/s, respectively Subrahmanyam et al. (2001). The phase speed of WPPW match well with that of the second-mode baroclinic Rossby wave. For the generation mechanics, Subrahmanyam et al. (2001) argued that this kind Rossby wave was probably radiated from coastal trapped Kelvin wave at south-west coast of Indian. Meanwhile, this kind Rossby wave can bring wave energy from south-west coast of Indian to the Somali coast, and feed the Somali Current and Somali eddies. The present study displays the vertical structure of this kind Rossby wave, however, the dynamics of WPPW (and Rossby wave) and the its association with Somali Current and Somali eddies call for further study. "

Page 7, line 7. Strictly speaking, the boundary between the tropics and the subtropics is around 23.5°N, so all of the observations being considered here are from the tropics. Consequently, the use of the word subtropical is misleading. Subsequent uses of these terms should also be revised.
Response: We corrected the statement accordingly. We changed the "tropical band" to "equatorial band", and changed the "subtropical band" to "tropical band" in the whole paper.

Page 7, line 7. I do not think the authors are justified in grouping PGW and RSW as RSPGIW. In Figure 2, the water masses are observed to be separate, and the authors have acknowledged the different densities of the two water masses.
Response: [Page 9, line 13–14, in change-track-mode revised manuscript] We deleted the statements related to RSPGIW.

Page 7, line 18. The observations from the World Ocean Atlas presented in Figure 3 are from a climatology and should not, therefore, be described as a snapshot.
Response: [Page 9, line 15, in change-track-mode revised manuscript] We corrected the statement.

Page 7, line 19. The authors have not marked north and south on Figure 3, so it is difficult for the reader to make sense of statements such as "the thermocline... deepens northward".
Response: [Page 19, Figure 4, in change-track-mode revised manuscript] We therefore added the latitude in Figure 3 (Figure 4 in revised manuscript).

Page 7, line 22. I do not really agree with the authors's point about ventilation. The outcropping of isotherms visible in Figure 3 is from within the mixed layer? it is not clear that "subsurface" water is then able to take part in air-sea interaction.
Response: We argue that the mixed-layer is approximately well-mixed bulk layer, which can be defined as the layer of temperature within SST minus 0.1 (or 0.5) °C. In Figure 3 (Figure 4 in revised manuscript), the interval of temperature contour is 1.0 °C, therefore, we suppose that the outcropping isothermal line was below the mixed-layer, and argue the "subsurface" water taken part in air-sea interaction.

Page 7, line 28. The authors do not explain why their observations show that saline intermedi-

ate waters are PGW and RSW ? nor do they explain why this is not clear in the climatology.
Response: [Page 9, line 28–29, in change-track-mode revised manuscript] Basically, we identified the PGW and RSW from T-S diagram. We added the reason in revised manuscript. For explain on the climatology, we added
"In other words, the comparison implies that the year 2002 is an anomaly year on the distributions of ASHSW, PGW and RSW."

Page 7, line 31. Why have the authors chosen the 22 kg m-3 isopycnal?
Response: We chosen 22 kg m-3 because it was the first near-surface isopycnal in climatology, meanwhile, and it characterized the differences among four datasets.

Page 7, line 33. It is hard to compare Figure 1b and Figure 3, because Figure 1b uses degrees and Figure 3 uses km.
Response: [Page 18, Figure 4, in change-track-mode revised manuscript] We added the latitude in the Figure.

Page 7, line 33. I do not understand what is meant by projecting the outcrop point in the wind vector field.
Response: [Page 9, line 32, in change-track-mode revised manuscript] We deleted "when we project the outcrop point in the wind vector field".

Page 8, Figure 2. I am not sure why the mean temperature-salinity curves have been plotted. They are not mentioned in the text and they distract from the new observations.
Response: [Page 10, Figure 3, in change-track-mode revised manuscript] We moved out the mean temperature-salinity curves.

Page 9, line 1. I don't think that the thermocline can be described as descending "sharply".
Response: [Page 11, line 1, in change-track-mode revised manuscript] We deleted "sharply".

Page 9, line 5. I don't understand what is "remarkable" about the southward extension of salty water.
Response: [Page 11, line 6, in change-track-mode revised manuscript] "the remarkable southward extension of salty water in the upper ocean"
is modified to
"the southward extent of ASHSW".

Page 9, line 15. Again, I don't understand why the velocity field in the upper ocean is "remarkable".
Response: [Page 11, line 16, in change-track-mode revised manuscript] We changed "remarkable" to "relatively strong".

Page 9, line 19. I think the authors need to label features of interest? eg CCE2 ? on Figure 4. As it stands, it is quite hard to see what the authors want the reader to look at.

Response: [Page 20 Figure 5, in change-track-mode revised manuscript] We added the position of CCE1, CCE2 and WPPW in the Figure.

Page 9, line 22. The authors need to discuss, somewhere in the paper, the significance of the westward-propagating disturbance. At the end of the paper, I have no better idea of what is it and why it might be significant than I had at the start.

Response: [Page 2 line 24-28, in change-track-mode revised manuscript] In the introduction section, we added:

"Besides, the planetary waves at-least include Rossby and Kelvin waves (Rhines, 1975; McCreary, 1985). Satellite-retrieved sea surface height are commonly used to detect the planetary waves (Chelton and Schlax, 1996), however, the internal dynamics of planetary wave is not sufficiently addressed. The phase speed of west-propagating planetary wave (WPPW) is used to match the theoretical Rossby wave, nonetheless, the vertical structure of WPPW calls for vertical profiling observation (Subrahmanyam et al., 2001)."

Page 9, line 26. When comparing the observationally derived geostrophic current and the current fields from the re-analysis products, have the authors considered that the current fields in the re-analysis products might contain ageostrophic components, eg Ekman flow?

Response: [Page 12 line 4–9, in change-track-mode revised manuscript] In section 3.3, we added a paragraph on discussion the Ekman flow:

"Part of the difference between observation-based absolute geostrophic current and reanalysis current is due to the near-surface Ekman current. The mean surface Ekman speed, which is approximately the difference between surface geostrophic current and in-situ surface current (from surface drifter), is within 0.1 m/s in northern IO (Saj, 2017). Besides, the climatological monthly mean mixed-layer depth in May is roughly 20 m at station 9.5°N and 59.5°E (on CR; Liu et al., 2018). Considering the near-surface Ekman current decays exponentially with depth, therefore, the near-surface Ekman currents in reanalysis datasets are relatively weak to affect the main results as mentioned above."

Page 10, first paragraph. I do not understand the argument that this paragraph is trying to make. There are several ideas that are not fully explored and which are insufficiently referenced. The authors seem to be contrasting "customary ventilation theory" and its corresponding meridional flow with "potential vorticity analysis" and its corresponding zonal flow. This strikes me as being a massive oversimplification; at the least, it requires a much more detailed explanation. Much of this material " as well as the extra explanation I would like to see added " probably belongs in the introduction.

Page 10, line 1. In what way are explanations of ASHSW and RSW pathways "ambiguous". This statement needs to be referenced, evidenced and more fully explained, either here or in the introduction.

Response: [Page 2 line 10-17, in change-track-mode revised manuscript] We moved the paragraph into the Introduction Section. We modified the explanation, as

"For instance, three water masses were defined in NWIO as Arabian Sea High-Salinity Water

(ASHSW), Persian Gulf Water (PGW) and Red Sea Water (RSW). Regarding the pathways of these water masses, the mechanics are not clear. RSW is formed near the northern side of the NWIO; therefore, according to the customary ocean ventilation theory, RSW sinks and moves southward along the isopycnal layer from the generation zone following the wind-driven current (Luyten et al., 1983). However, the applicability of the ocean ventilation theory is still unknown for the northern IO, because the surface wind reverses direction under the influence of winter monsoon (Liu et al., 2018). Meanwhile, the limited meridional extent of IO omits the polar-to-subpolar front, which helps form intermediate water in Pacific and Atlantic Oceans (You, 1998). In contrast, in situ potential vorticity analysis on RSW reveals that the flows generally follow the zonal direction (Beal et al., 2000). How the water mass moves is worthy further investigation."

Page 10, line 5. This sentence is poorly expressed.

Response: [Page 2 line 14-18, in change-track-mode revised manuscript] We moved the paragraph into the Introduction Section. We changed

"However, the feasibility of the ocean ventilation theory is still under debate, especially for the northern IO, whose meridional extent is limited compared with the other two basins. "

into

"However, the applicability of the ocean ventilation theory is still unknown for the northern IO, because the surface wind reverses direction under the influence of winter monsoon (Liu et al., 2018). Meanwhile, the limited meridional extent of IO omits the polar-to-subpolar front, which helps form intermediate water in Pacific and Atlantic Oceans (You, 1998). "

Page 10, second paragraph. The authors should explain clearly why they break up the particle tracking results into latitudinal bands? is this because they suspect different processes/currents are causing differences in circulation between these bands? Also, this paragraph should make some attempt to elucidate these processes and to explain what's new and important about these results. At present, the text just explains what the reader can already see in the figure.

Page 10, line 14. I do not agree that this looks like flow in the summer Somali Current.

Response: [Page 12, line 21 – Page 13 line 2, in change-track-mode revised manuscript] We revised the paragraph. We added:

"For better describing the trajectories, we separate the CR to three latitude bands as 2.3-5°N (equatorial band), 5-8°N and 8-9.8°N."

"In the equatorial band (Fig. 6e), the near-equator tracers come from the west side, which is consistent with the north branch of East African Coastal Current during summer monsoon (Schott and McCreary Jr., 2001; Schott et al., 2009)."

"Meanwhile, for the relatively north-side tracers in equatorial band, the trajectories backtrack to east side, which is probably following a westward current or meso-scale eddy."

"For latitudes from 8-9.8°N (Fig. 6a), the trajectories emphasis the north branch of East

African Coastal Current, meanwhile, the water at the north station of CR comes from the northeast side, and one station water shows the cross-equatorial current around 53°E (east of Southern Gyre; Schott et al., 2009). "

Accordingly, we deleted:

"For the tropical band (Fig. 6e), the water mainly follows the zonal movement, but the near-equator tracers are from west side and relatively north-side tracers come from east side."

"For latitudes from 8-9.8°N (Fig. 6a), the trajectories look like the flow of the summer Somalia Current (Schott et al., 2009)"

Page 10, third paragraph. Again, some discussion of processes is needed here.

Response: [Page 13, line 3–15, in change-track-mode revised manuscript] We rewritten the paragraph. Original version:

For the RSW in the intermediate-depth layer at 700 m, the trajectories in the tropical band (Fig. 6f) and at latitudes from 5-8°N (Fig. 6d) generally follow the zonal movement (Beal et al., 2000). The tracer movements at latitudes from 8-9.8°N (Fig. 6b) partly agree with those of the ventilation theory, and partly follow the zonal direction (Beal et al., 2000).

New version:

For the RSW in the intermediate-depth layer at 700 m, the trajectories in the equatorial band (Fig. 6f) show the zonal movement. Most of the trajectories move from the west side, which coincident with the potential vorticity explanation (Beal et al, 2000), that the RSW moves southward along the coast with the help of winter monsoon, and then leave the coast and shift to middle ocean via zonal movement. Other two trajectories come from east side, and one extra trajectory moves from northwest with circular track. Hence, these trajectories display three kinds of pathways. Accordingly, in the 5-8°N band (Fig. 6d), the mainly eastward zonal movements agree with (Beal et al., 2000), meanwhile, some westward trajectories resemble the ventilation theory (Luyten et al., 1983; Qiu and Huang, 1995). At last, in the 8-9.8°N (Fig. 6b), new pathway directly from northwest is emerged, and the trajectories support 700 m waters are probably directly from east of the Horn of Africa (or Gulf of Aden) without southward movements along the coast.

Page 10, line 25. Are there papers or technical reports available that explain methodological differences between the HYCOM and SODA re-analyses? Would more thorough research negate the need for speculation?

Page 10, line 27. It is not clear to me what is meant by the "dynamic core" of the ocean general circulation model.

Response: [Page 13, line 26– Page 14 line 4, in change-track-mode revised manuscript] We nearly rewritten the paragraph. We changed

"We speculate that although both SODA and HYCOM assimilate the Argo data into an Oceainc General Circulation Model (OGCM), the methodology of assimilation or the weight between OGCM and in situ observations, is sharply different. We assume the southward extension of ASHSW could be simulated by the dynamic core of OGCM, and the phenomenon was not cap-

tured in the Argo-only observation, therefore, HYCOM seems more to approach the dynamic model, and SODA weighted more on the Argo-only observations. Additionally, the finer horizontal resolution of HYCOM likely helps HYCOM involve more physically sound mechanics, such as the downwelling of salty water and wind-driven meridional movement."
to
"Although both SODA and HYCOM assimilate the Argo data into Oceainc General Circulation Models (OGCMs), the assimilation methods of SODA and HYCOM are considerably different. SODA adopts optimal interpolation (Carton et al., 2008), while HYCOM uses 3D variational scheme. One advantage of 3D variational scheme versus optimal interpolation is the conservation of dynamical constraints (Zhu et al., 2006; Yin et al., 2012; Edwards et al., 2015). Therefore, HYCOM probably describes better on the wind-driven circulations, monsoon-induced coastal current and meso-scale eddy movement, which are all related to the southward extension of ASHSW."

Page 10, line 33. I dislike the description of geostrophic current as an "alternative result for the ocean current". Geostrophic flow is an important part of ocean circulation and is perfectly valid in its own right.
Response: [Page 14, line 5-7, in change-track-mode revised manuscript] The sentences were deleted.

Page 11, conclusions section. The particle tracking results are not mentioned in the conclusion.
Response: [Page 15, line 12–16, in change-track-mode revised manuscript] We added paragraph in conclusion section, as
"To explore the pathways of ASHSW and RSW during the expedition time, we set tracers in SODA dataset at depths of 100 and 700 m, and backtrack their trajectories via three dimensional Lagrangian description. Overall, for the 100 m depth waters, the results reveal the pathways related to the north branch of East African Coastal Current and the flow from northeast side (or Arabian Basin), while for the 700 m depth waters, the trajectories mainly follow the zonal direction from either west and east sides. The results give direct-viewing descriptions and call for further dynamical investigations."

Page 11, line 2. The authors have not discussed baroclinic modes in the results section, so it does not make any sense to the reader when the concept is introduced in the discussion section. Furthermore, are the authors certain that baroclinic mode is an appropriate concept in this instance?
Response: [Page 13, line 18, in change-track-mode revised manuscript] We changed the word "baroclinic mode" into "vertical structure".

Page 11, line 11. It is not correct to say that you integrate density to get the geostrophic current.
Response: [Page 14, line 32, in change-track-mode revised manuscript] We changed
"we integrate the density field to obtain the absolute geostrophic current."

into

"we compute the absolute geostrophic current based on the density profiles and sea surface height".

Page 11, line 20. I do not think that the authors have shown how "the present analysis shows potential data applications for the future".

Response: [Page 15, line 7–9, in change-track-mode revised manuscript] We changed

"The present analysis shows potential data applications for the future, where the meso-scale eddies are relatively important but cannot be well described by the Argo-only data source."

into

"Over the NWIO, the meso-scale eddies are relatively important but cannot be well described by the Argo-only data source. The present analysis shows more data source for potential data assimilation experiment."

Page 14, Figure 3. Using km as the horizontal co-ordinate is unhelpful, given that in the text what is actually interesting is the location in degrees north. The authors should also mark on features of interest discussed in the text, such as the eddies.

Response: [Page 19, Figure 4, in change-track-mode revised manuscript] We added the latitude in the Figure.

Page 16, Figure 5. Given that the westward-propagating disturbance is so little discussed, I do not think that this figure adds anything to the paper.

Response: We removed this figure.

Hydrographic survey over the Carlsberg Ridge in May 2012

Hailun He[1], Yuan Wang[2], Xiqiu Han[2], Yanzhou Wei[1], Pengfei Lin[3], Zhongyan Qiu[2], and Yejian Wang[2]

[1]State Key Laboratory of Satellite Ocean Environment Dynamics, Second Institute of Oceanography, Ministry of Natural Resources, Hangzhou 310012, China

[2]Key Laboratory of Submarine Geosciences, Second Institute of Oceanography, Ministry of Natural Resources, Hangzhou 310012, China

[3]State Key Laboratory of Numerical Modeling for Atmospheric Sciences and Geophysical Fluid Dynamics, Institute of Atmospheric Physics, Chinese Academy of Sciences, Beijing 100029, China

Correspondence: Hailun He (hehailun@sio.org.cn); Xiqiu Han (xqhan@sio.org.cn)

Abstract. In May 2012, we conducted a hydrographic survey over the Carlsberg Ridge in the northwest Indian Ocean. In this paper, we use these station data, in combination with some free-floating Argo profiles, to obtain the sectional temperature and salinity fields, and subsequently, the hydrographic characteristics are comprehensively analyzed. Through the basic T-S diagram, three salty water masses, Arabian Sea High-Salinity Water, Persian Gulf Water, and Red Sea Water, are identified. The sectional data show a clear ventilation structure associated with Arabian Sea High-Salinity Water. The 35.8 psu salty water sinks at 6.9°N and extends southward to 4.4°N at depths around the thermocline, where the thermocline depth is in the range of 100 to 150 m. This salty thermocline extends much further south than the climatology indicates. Furthermore, the temperature and salinity data are used to compute the absolute geostrophic current over the specific section, and the results show meso-scale eddy vertical structure different from some widely used oceanic reanalysis data. We also find a west-propagating planetary wave ~~disturbance~~ at 6°N, and the related features are described in terms of phase speed, horizontal and vertical structures.

1 Introduction

The northwest Indian Ocean (NWIO) is unique compared with the other two basin-scale oceans (Pacific and Atlantic Oceans) because the dominant characteristics are monsoon driven (Schott and McCreary Jr., 2001; Schott et al., 2009). The seasonal monsoon forces the coastal current back and forth and generates the ~~renewed~~ Somalia Current, which is always marked as the strongest current in the real ocean (as strong as 3.5 m s^{-1}). Moreover, the monsoon is strong to change the pattern of basin-scale circulation. T~~t~~he monsoon builds up a dominant meridional current in the NWIO, ~~which~~ changing the form of the customary zonal current (as in the Pacific and Atlantic Oceans) into a ~~the~~ meridional current. NWIO is also famous for its role in the so-called Indian Ocean Dipole (IOD; Saji et al., 1999; Webster et al., 1999; Han et al., 2014; Chen et al., 2015), which represents the zonal gradient of sea surface temperature (SST) in the Indian Ocean (IO). As a basin-wide signal, the IOD is closely related to the IO-adjacent climate (Li and Han, 2015). Some studies also emphasized the distinct meso- and submeso-scale air-sea interactions in the NWIO (Vecchi et al., 2004).

~~Historically, the John Murray/Mabahiss expedition (1933-1934) was an early one-time IO exploration. Later, the First International Indian Ocean Expedition (IIOE-1; 1962-1965) and the subsequent Second International Indian Ocean Expedition~~

~~(IIOE-2; 2015-2020) were marked by famous international cooperation (Wooster, 1984; Aleem and Morcos, 1984; Hood et al., 2016). Between IIOE-1 and IIOE-2, the World Ocean Circulation Experiment (WOCE, 1990-1997; Ganachaud and Wunsch, 2000, 2003) defined ten one-time sections and three repeated sections in the IO (Talley, 2013). Next, considering the importance of continuous time series data, Research Moored Array for African-Asian-Australian Monsoon Analysis and Prediction (RAMA) was implemented in the tropical Indian Ocean and delivered fixed-position environmental parameters. Also, the implementation of the Array for Real-time Geostrophic Oceanography (Argo) project advanced the sampling process to be automatic and near real-time (Yin et al., 2012).~~

To date, the main water masses in the IO and NWIO have been described ~~are understood~~ by the scientific community (Sharma et al., 1978; Kumar and Prasad, 1999; Emery, 2001; Talley et al., 2011)~~, although some regional water masses and their short-term variations are still not well documented~~. For instance, three water masses were defined in NWIO as Arabian Sea High-Salinity Water (ASHSW), Persian Gulf Water (PGW) and Red Sea Water (RSW). Regarding the pathways of these water masses, the mechanics are not clear. RSW is formed near the northern side of the NWIO; therefore, according to the customary ocean ventilation theory, RSW sinks and moves southward along the isopycnal layer from the generation zone following the wind-driven current (Luyten et al., 1983). However, the applicability of the ocean ventilation theory is still unknown for the northern IO, because the surface wind reverses direction under the influence of winter monsoon (Liu et al., 2018). Meanwhile, the limited meridional extent of IO omits the polar-to-subpolar front, which helps form intermediate water in Pacific Ocean and Atlantic Ocean (You, 1998). In contrast~~For instance~~, in situ potential vorticity analysis on RSW reveals that the flows generally follow the zonal direction (Beal et al., 2000). How the water mass moves is worthy further investigation.

On the other hand, the meso-scale eddies and planetary waves are not sufficiently observed in NWIO. The historical and present Research Moored Array for African-Asian-Australian Monsoon Analysis and Prediction (RAMA) ~~RAMA~~ observation arrays are close to the equator ~~tropic~~ and omit the NWIO. In situ observations in the NWIO mainly depend on Array for Real-time Geostrophic Oceanography (Argo; Riser et al., 2016; Vitale et al., 2017). However, as we show later, the number of Argo floats is still too sparse to represent the meso-scale eddy field in the NWIO. ~~The present circumstance stimulates our effort to find more observational resources.~~ Besides, the planetary waves at-least include Rossby and Kelvin waves (Rhines, 1975; McCreary, 1985). Satellite-retrieved sea surface height are commonly used to detect the planetary waves (Chelton and Schlax, 1996), however, the internal dynamics of planetary wave is not sufficiently addressed. The phase speed of west-propagating planetary wave (WPPW) is used to match the theoretical Rossby wave, nonetheless, the vertical structure of WPPW calls for vertical profiling observation (Subrahmanyam et al., 2001).

The present circumstance stimulates our effort to find more observational resources. The Carlsberg Ridge (CR) is a typical slow-spreading ridge and lies along the northwest-southeast direction in the NWIO. Recently, we conducted an interdiscriplinary ~~interdiscripline~~ survery on CR (Yang et al., 2016; Wang et al., 2017)~~, and the CTD and XCTD station data have not yet been explored.~~ , and the hydrographic ~~Hydrographic~~ analysis of CR is necessary for at least three reasons. First, hydrographic survey takes a snapshot on the water mass, and gives an evidence on the activity of water mass. Second, the observation probably captures the vertical structure of meso-scale eddy or planetary wave. Third, the results could be used to evaluate the widely-used oceanic reanalysis. ~~First, such analysis helps us to define regional ocean circulation and regional~~

~~multiscale air-sea interactions. Second, the analysis supplies basic environmental parameters to determine the movements of sporadic hydrothermal activity. Third, this analysis sheds new light into the basic energy theory of ocean circulation (Huang, 1999).~~ The trajectory of Argo float are not manually controlled; however, ship surveys could cover specified sections and have a clearer objective. Hence, this paper aims to analyze hydrographic information by combining both CR expedition and Argo floats.

2 Data and methods

2.1 In situ data description

The data for our study were collected during the Chinese cruise DY125-24 (May 2012) by the Chinese research vessel "LISIGUANG". Hydrographic observations were conducted in the region of the CR ~~Carlsberg Ridge~~. The vertical profiles of temperature, conductivity and pressure were obtained by a calibrated SBE-19plus CTD and some expendable CTD (XCTD). The station information is shown in Fig. 1 and Table 1. All stations were mainly located along the CR section and therefore defined the regional along-section (y) and cross-section (x) coordinates. The maximum measurement depths of XCTD and Argo are 1050 and 2000 m, and therefore we limited our analysis to depth 2000 m. According to Talley et al. (2011) and Emery (2001), upper 2000 m depth covers the upper ocean (defined as 0-500 m) and the intermediate-depth ocean (defined as 500-2000 m).

Regarding data quality, an intercomparison between XCTD and CTD measurement was implemented in the southern tropical Indian Ocean. The XCTD station involved was located at 73.8°E and 1.7°S at 14:23 on May 4 (Coordinated Universal Time), and the counterpart CTD station was located at 73.5°E and 1.4°S a half-hour later (14:58 on May 4; distance with the XCTD station as 47.17 km). The mean differences in the recorded in situ temperature (salinity) were 0.425°C (0.058 psu) in the upper ocean and 0.051°C (0.053 psu) in the intermediate-depth ocean.

In our postprocessing, 13 simultaneous Argo profiles were found within a 200 km radius of the study region (Fig. 2 and Table 1). The Argo float is free-floating without regular calibration; therefore, quantifying the uncertainty ~~bias~~ of Argo is relatively important before using the data. Fortunately, an Argo float drifted (2900877) around an XCTD station (S20CTD16; Table 1; distance with the Argo float as 79.97 km), and the two measurements occurred on May 17 and May 16, respectively. Then, we compared the XCTD with the Argo profile, and the mean differences in the in situ temperature (salinity) were 0.076°C (0.144 psu) in the upper ocean and 0.374°C (0.171 psu) in the intermediate-depth ocean. It is also noted that the differences for temperature and salinity in the intermediate depth ocean are much larger than those in the upper ocean, which is probably due to the oceanic internal high-wavenumber signals between two stations. Differences among CTD, XCTD and Argo are not negligible. However, because the distances between two stations in comparisons are relatively large, and the biases of XCTD and Argo are different for instruments, we does not perform instrument calibration. We later use objective analysis method and low-pass filter to smooth the data among CTD, XCTD and Argo.

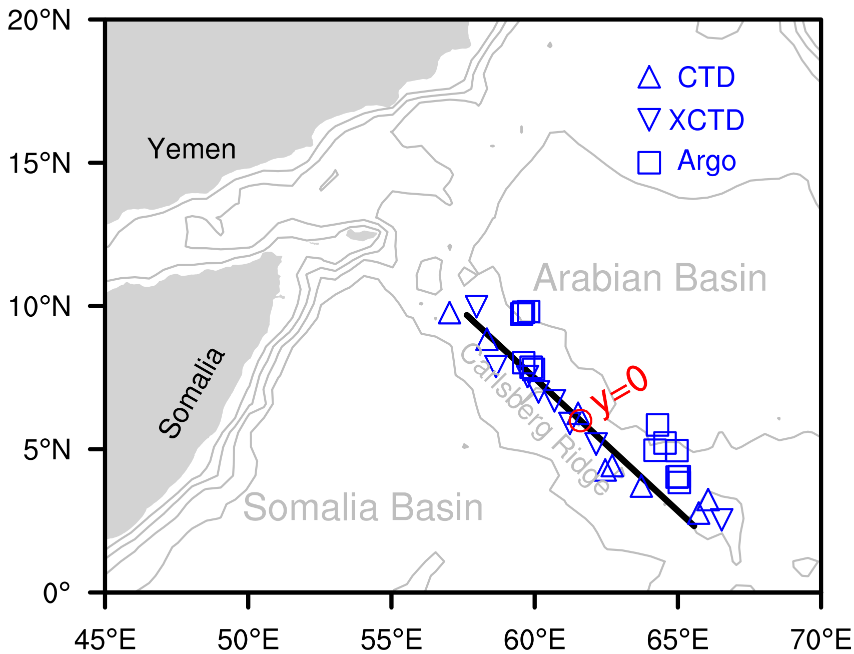

Figure 1. CTD/XCTD stations of the DY125-24 survey and the simultaneous Argo profiles around the CR. The CR defines local coordinates in which the x-coordinate is cross-track and the y-coordinate along-track, the corresponding origin point is selected as (61.6°E, 6.0°N), and the isobaths of -4000, -3000, -2000 and -1000 m are presented.

2.2 In situ data processing

All the data from several sources need to be processed to same levels because of the different sampling rates; i.e., the vertical resolutions of CTD, XCTD and Argo are 0.1, 0.1, and 2.0 m, respectively. In the first step of data postprocessing, the coarse data are moving-averaged into a uniform vertical grid with a 5 m interval starting from 5 m below the surface. Here 5 m vertical resolution is sufficient for describing vertical structure of mixed-layer and water masses. Special treatment is imposed on one Argo float (2901888; three profiles; Table 1), where the coarse profiles lose data in the upper 20 m; thus, the missing data are filled with the same value as uppermost available data in the near surface.

The data are then projected into the standard CR section (y-coordinate), and the corresponding grid interval is 50 km. ~~, with a uniform 100 km interval in the y-coordinate.~~ We use the objective analysis method to interpolate data from irregularly spaced locations to a fixed grid (Barnes, 1994). Later, a low-pass filter is imposed on the CR sectional data to remove the short-wavelength signals, which are partly from the cross-bias among different data sources and partly from the submesoscale or higher wavenumber signals in the real ocean. The low-pass filter is a two-dimensional LOcally Estimated Scatterplot Smooth-

Table 1. Information on CTD/XCTD stations and Argo floats.

Type	Station/Float	Latitude	Longitude	Time (month/day hour)
XCTD	S09CTD08	2.3°N	66.3°E	05/06 07
XCTD	S16CTD13	5.1°N	62.1°E	05/14 16
XCTD	S19CTD15	6.4°N	60.4°E	05/16 13
XCTD	S20CTD16	7.3°N	59.5°E	05/16 19
XCTD	S23CTD19	7.0°N	60.1°E	05/20 14
XCTD	S25CTD21	9.6°N	57.6°E	05/23 04
XCTD	S26CTD22	5.5°N	61.1°E	05/26 20
CTD	S10CTD09	3.1°N	66.0°E	05/07 05
CTD	S12CTD10	2.5°N	65.4°E	05/09 12
CTD	S14CTD11	4.2°N	62.3°E	05/11 17
CTD	S15CTD12	4.3°N	62.4°E	05/13 21
CTD	S17CTD14	6.2°N	61.3°E	05/15 08
CTD	S21CTD17	8.5°N	58.2°E	05/17 05
CTD	S22CTD18	9.5°N	57.0°E	05/18 07
CTD	S28CTD24	3.4°N	63.4°E	06/01 04
Argo	2901847	4.0°N	65.0°E	05/03 02
Argo	2901848	5.8°N	64.3°E	05/07 13
Argo	2900877	8.0°N	59.6°E	05/07 09
Argo	2901096	5.0°N	64.2°E	05/08 19
Argo	2901888	9.7°N	59.5°E	05/08 01
Argo	2901847	4.0°N	65.0°E	05/12 20
Argo	2901888	9.8°N	59.6°E	05/17 23
Argo	2900877	7.9°N	59.9°E	05/17 09
Argo	2901096	5.2°N	64.6°E	05/18 19
Argo	2901847	3.8°N	65.1°E	05/22 16
Argo	2900877	7.8°N	60.0°E	05/27 09
Argo	2901096	5.0°N	65.0°E	05/28 18
Argo	2901888	9.8°N	59.8°E	05/28 01

ing (LOESS) filter (Cleveland and Grosse, 1991), and the moving-average wavelengths are 300 km and 30 m in the horizontal and vertical directions, respectively. As a result, the smoothed data save the essential features of the thermal-salinity field but remove the noise.

2.3 Satellite data description

2.3.1 Surface wind

We use Cross-Calibrated Multi-Platform (CCMP; Atlas et al., 2011) gridded surface vector winds here (version 2.0). CCMP data are daily products, and they are projected on 0.25°×0.25° grids.

2.3.2 Sea surface temperature

The sea surface temperature (SST) data is produced by Operational Sea Surface Temperature and Sea Ice Analysis (OSTIA; Donlon et al., 2011), which merges satellite infrared and microwave products, ship, buoy, etc. OSTIA is daily product, and the horizontal resolutions are 0.05°×0.05°.

2.3.3 Sea surface height

For describing the sea surface height (SSH) and the related surface geostrophic current, we use the Archiving, Validation, and Interpretation of Satellite Oceanographic (AVISO) grided data. The temporal resolution is daily, and the horizontal resolutions are 0.25°×0.25°.

2.4 Reanalysis data description

As references, we also employ two widely used reanalysis datasets for comparison, aiming at evaluating the quality of reanalysis data. The first reanalysis dataset is Simple Ocean Data Assimilation (SODA, version 3.3.1; Carton and Giese, 2008; Carton et al., 2018), whose horizontal resolutions are 0.25°×0.25° for longitude and latitude. The second reanalysis dataset is HYbrid Coordinate Ocean Model (HYCOM, version GOPS3.0:HYCOM+NCODA global 1/12° Reanalysis GLBu0.08/expt_19.1), and its horizontal resolutions are 0.08°×0.08°. Both SODA and HYCOM assimilate various in situ and satellite-based data sources: historical station profiles, Argo profiles, moorings, drifters, satellite SSTs, SSHs, etc. For comparison, we extract the reanalysis datasets along the same section as the observations, and the monthly mean fields are used.

2.5 Method of tracers

Using SODA reanalysis, we release some passive tracers along the CR and backtrack their trajectories based on the Lagrangian description, and the methods are formulated by

$$\begin{cases} X^{n-1/2} & = X^{n+1/2} - U^n \cdot \Delta t \\ Y^{n-1/2} & = Y^{n+1/2} - V^n \cdot \Delta t \\ z^{n-1/2} & = z^{n+1/2} - w^n \cdot \Delta t \end{cases} \tag{1}$$

Here, X and Y are the Cartesian coordinates along longitude and latitude respectively, U and V are the corresponding currents, z is the vertical coordinate, w is the vertical velocity, and n is the time step. In the computation, we use the three dimensional velocity (U, V, w) to track the tracers, and we set the ~~interval of~~ time step (Δt) as 3600 s. The tracers are set along the CR on May 15, 2012, and then backward integrated to January 1, 2010.

3 Results

3.1 Background environment

The time period of the shipboard survey starts ~~start~~ from 2012/05/06 and ends ~~end~~ at 2012/06/01 (Table 1). Figure 2(a-c) ~~1(b-d)~~ show the monthly mean surface wind, SST and SSH, respectively. In this specific month, ~~which is preferentially defined as the later stage of monsoon transition,~~ the summer monsoon has started but is not very strong (Fig. 2a ~~1b~~) . The along-coast wind prevails in the regional wind field, and the wind speed in the region far from the western coast is weaker. Positive wind curl along the Somalia coast and Yemen ~~is responsible for off-coast Ekman water transport, which~~ induces sufficient coastal upwelling , which brings ~~to bring~~ lower-layer cold water upward and cools ~~cool~~ the sea surface (Fig. 2b ~~1c~~). The patterns of wind curl are roughly consistent with that of the climatological monthly mean wind stress curl (Beal et al., 2013)~~, where the wind stress curl highlights the strong seasonal variations, particularly along the Arabian Peninsula.~~ Otherwise, the dominant wind curl in the NWIO is negative, which is consistent with the annual mean, and forces downwelling ~~denote the downwelling-preferred wind-forcing circumstance~~. ~~Wind and SST have a close relationship (Fig. 1c). The near-coast Ekman pumping generates a sharp SST front at the transition area between the coast and oceanic interior.~~ The basin-scale semicircular SST contour (30°C) ~~front~~ then outlines a warm area in the oceanic interior~~, where SST exceeds 30°C~~. The main part of the CR is located in this strikingly warm region (Fig. 2b).

On the other hand, SSH (or absolute dynamic height, ADT) shows multiple meso-scale eddies (Fig. 2c ~~1d~~). There are some warm-core eddies (anti-cyclonic eddies), to the east of the CR (WCE1), east of the Horn of Africa (WCE2), and northeast of the Horn of Africa but very close to Yemen (WCE3). ~~The first two warm-core eddies (WCE1 and WCE2) seem to release footprints in the wind stress curl (Fig.1b); however, WCE3 does not induce significant wind curl anomalies.~~ Two cold-core eddies (cyclonic eddies; CCE1 and CCE2) are also observed at either end of the CR. Besides, a remarkable westward current is observed at the latitude of 6°N, which is noted here as a WPPW ~~westward-propagating disturbance (WPD)~~. WPPW ~~WPD~~ is pronounced compared with the circumstances around the specific region, which refers to the zonal extent (7.5° in longitude), while the meridional extent is relatively narrow (1.3° in latitude). The magnitude of zonal current is -0.38 m/s. ~~which refers to not only the magnitude (-0.38 m/s for the zonal current) but also the zonal extent (7.5° in longitude), although its meridional extent is relatively narrow (1.3° in latitude).~~ Furthermore, we investigated the longitude-time plot of the surface zonal current at 6°N latitude (surface geostrophic current from SSH; results are not shown here), the WPPW~~WPD~~ is observed to start at 69°E on day 102, the surface current propagates westward with a phase speed of 0.2 m s^{-1} and arrives at 60°E on day 155.

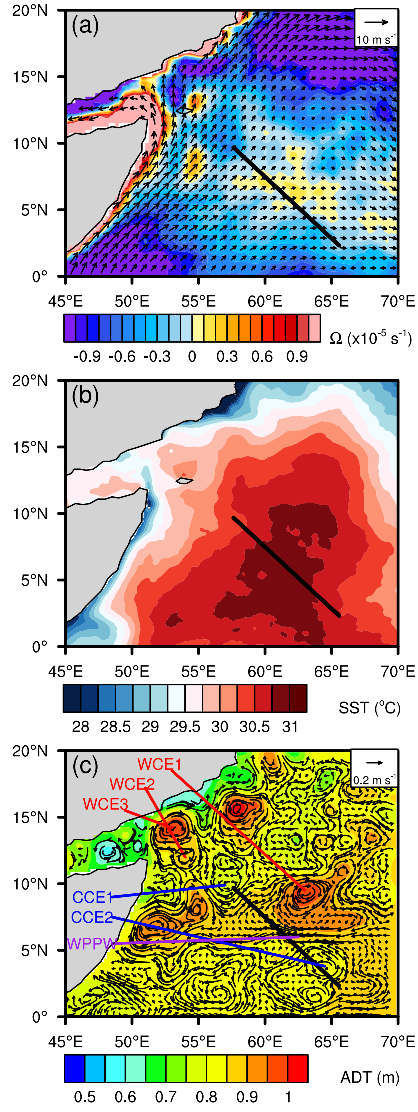

Figure 2. ~~(a) CTD/XCTD Stations of the DY24 survey and the simultaneous Argo profiles around the CR. The CR defines local coordinates in which the x-coordinate is cross-track and the y-coordinate along-track, the corresponding origin point is selected as (61.6°E, 6.0°N), and the isobaths of -4000, -3000, -2000 and -1000 m are presented;~~ (a) ~~(b)~~ monthly mean wind vector and vorticity (Ω) from CCMP wind data, data are plotted every 3 points for wind vector~~, the positive and negative vorticities are displayed by red and blue contours repectively~~; (b)~~(c)~~ monthly mean sea surface temperature from OSTIA data; and (c)~~(d)~~ monthly mean sea surface height (absolute dynamic topography), and the consistent surface geostrophic current (shown with every 2 points) from AVISO.

3.2 Temperature, salinity and density

First, we impose the water mass analysis on the objective-analysis data (section 2.2), and the results are shown in Fig. 3. The data support that the upper water is more saline than the Indian Equatorial Water (IEW) and fresher than the Arabian Sea Water (ASW). The observed waters are likely to be mixed IEW and ASW. When the latitude spans from the equatorial ~~tropical~~ band (2.3-5°N in the present study) to the tropical ~~subtropical~~ band (5-9.7°N in the present study), the salinity generally increases, consistent with the northern-side ASW being much more saline than the southern-side IEW (Han et al., 2014) and this meridional variation in salinity is due to the different proportions of IEW and ASW. On the northwest side, water columns contain ASHSW ~~Arabian Sea High-Salinity Water (ASHSW)~~, which are observed as saline water at a potential density of approximately 24 kg/m^3 (Kumar and Prasad, 1999).

The intermediate waters ~~(500 - 1500 m)~~ from our data are projected as PGW (Prasad et al., 2001) ~~Persian Gulf Water (PGW, Prasad et al., 2001)~~ and RSW (Beal et al., 2000; Talley et al., 2011) ~~Red Sea Water (RSW, Beal et al., 2000; Talley et al., 2011)~~. According to Kumar and Prasad (1999), the definition of PGW (RSW) is the density range as 26.2-26.8 kg/m^3 (27.0-27.4 kg/m^3), temperature range 13-19°C (9-11°C), and the salinity range 35.1-37.9 psu (35.1-35.7 psu). ~~Despite RSW is deeper than PGW, both PGW and RSW are defined as Red Sea-Persian Gulf intermediate water (RSPGIW; Emery, 2001).~~

Sectional profiles ~~snapshots~~ of temperature and salinity are shown in Fig. 4. The thermocline is in the depth range of 100 to 150 m (20°C isothermal line, Xie et al., 2002). From the present observation ~~snapshot~~, the thermocline is nearly flat at the equatorial ~~tropical~~ band and deepens northward in the tropical ~~subtropical~~ band. This phenomenon is also supported by the climatological data, which reveal that the sectional distribution of the thermocline is similar to a long-standing geostrophic balanced signal. In the near surface, the isothermal line of 30°C rises ~~some isothermal lines rise~~ to the surface on the northern side and show a clear ventilation structure such that subsurface water can take part in the air-sea interaction. Meanwhile, for the intermediate water, the isothermal line tilts deeper from south to north.

The striking feature of the salinity field is that a salinity tongue appears at 100 m depth, where the salty water is ASHSW (Kumar and Prasad, 1999). Climatological data show that these salty waters originate from the north side and extend southward; however, in our survey, the extent is greater. We emphasize the iso-salinity line of 35.8 psu; the southern extension can reach y=150 km (or 6.9°N) in climatology but -250 km (or 4.4°N) in our survey. This result means that the salty water extends southward more than 2.5° in latitude in excess of climatology. The present observation also shows the salty intermediate water as PGW and RSW (Fig. 3). The observation shows slightly more saline water than climatology on the northern side, although the overall structure is mostly consistent with the climatology. In other words, the comparison implies that the year 2002 is an anomaly year for the distributions of ASHSW, PGW and RSW.

When we move forward to the potential density field, the appearance of the 22 kg/m^3 isopycnal is evident in both the snapshot and climatology. For the snapshot, the outcrop point of the 22 kg/m^3 isopycnal is y=300 km, or 7.8°N. It is worth noting that the outcrop point is near the transition point for signs of wind vorticity ~~when we project the outcrop point in the wind vector field (Fig. 1b)~~ (Fig. 2a) , and the results suggest that the ventilation is induced by surface wind. The north side of

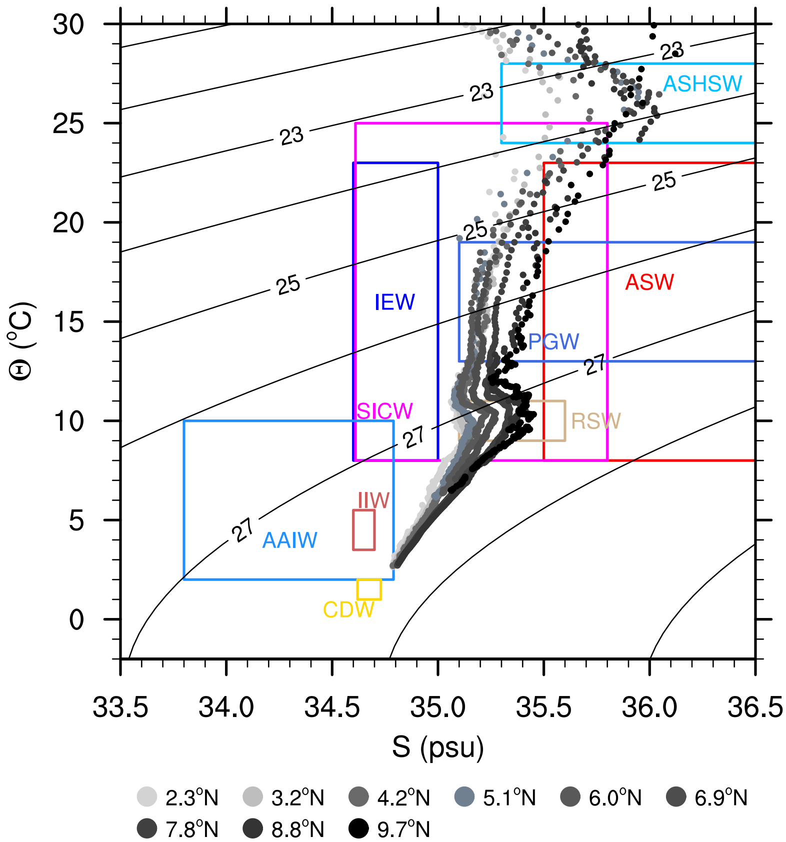

Figure 3. T-S diagram for the upper 2000 ~~1050~~ m of water on the CR. The water masses are defined in Emery (2001) and include the Arabian Sea water (ASW), Indian equatorial water (IEW), South Indian central water (SICW), Antarctic intermediate water (AAIW), Indonesian intermediate water (IIW), ~~Red Sea-Persian Gulf intermediate water (RSPGIW),~~ and circumpolar deep water (CDW). ~~The color lines are the mean T-S curves (Figure 8 in Emery (2001)), and t~~The rectangles represent the appropriate temperature and salinity ranges (Table 1 in Emery (2001)). Besides ~~In addition~~, Red Sea water (RSW), Persian Gulf water (PGW), and Arabian Sea High-Salinity Water (ASHSW) are also represented ~~in the present analysis~~ according to Kumar and Prasad (1999).

the outcrop point has negative wind vorticity, which promotes downwelling. Ventilation is highly related to the downwelling of high-salinity water and its southern extent ~~extension~~ (Luyten et al., 1983).

Fig. 4 also shows the reanalysis data, and essentially, the reanalysis captures the thermal structure quite well compared with the present observations and climatology. For instance, in the upper ocean, the surface warm water is distributed on the south side and northward to y=400 km where the isothermal line of 30°C ~~it~~ crops out. The observed ~~sharply~~ descending thermocline near y=100 km is recognizable ~~reproduced~~ in SODA and HYCOM. It is also noted that the equatorial ~~tropical~~ near-surface upwelling in HYCOM has some evidence from the present observations. For the intermediate-depth water, in SODA and HYCOM, the isothermal lines also tilt deeper from south to north, which resembles both the present observations and the climatology.

For salinity, the southward extent of ASHSW ~~remarkable southward extension of salty water in the upper ocean~~ is also captured by SODA and HYCOM, and the southward extent ~~extension~~ in HYCOM approaches the observations more closely. In the intermediate-depth water, the southward extent ~~extension~~ from the north side in SODA is similar to the observations, while the corresponding signal in HYCOM is obscured.

The upper ocean density fields from SODA and HYCOM also show clear ventilation structures. From the observations, equatorial ~~tropical~~ waters with a potential density of 22 kg/m^3 at a depth of 30 m are rising to the surface. The outcrop points of ~~a~~ potential density of 22 kg/m^3 in SODA and HYCOM are shifted southward compared with the observations. Additionally, the near-surface upwelling in the equatorial ~~tropical~~ band in HYCOM is strong, but not significant in the observations.

3.3 Cross-track current

The geostrophic current is deduced from the in situ density field by thermal wind theory (Fig. 5), where the velocity is integrated downward from the surface geostrophic current (Lagerloef et al., 1999). The velocity field is relatively strong ~~remarkable~~ in the upper ocean, where the current field is dominated by meso-scale eddies. The cross-track current in the equatorial ~~tropical~~ band is induced by CCE2. The structure of CCE2 is asymmetric, and the positive cross-track flow is stronger than the negative counterpart. In contrast, the northwest side of CR is identified as the south part of CCE1 (northeastward flow). ~~In contrast, the subtropical band is identified as the margin of a warm-core eddy, which is located northwest of the CR.~~ At 6°N latitude, the vertical structure of WPPW~~WPD~~ is well rebuilt in Fig. 5a. WPPW~~WPD~~ seems to extend vertically to a depth of 200 m, and the horizontal extent is near 200 km for the current greater than 0.02 m/s. Meanwhile, the maximum cross-track current of the WPPW~~disturbance~~ is 0.12 m/s. ~~Furthermore, Fig. 6 is the Hovmöller plot of the surface zonal current at 6°N latitude (surface geostrophic current from SSH). The WPD are observed to start at 69°E on day 102, propagate westward with a phase speed of 0.2 m s^{-1} and arrive at 60°E on day 155.~~ The current field also captures the northeastward ~~northeast~~ current (less than 0.075 m/s) in the intermediate depth (-200 $\leq y \leq$ -20 km, and 150 $\leq y \leq$ 350 km), which is due to the corresponding isothermal tilting (Fig. 4).

For the reanalysis data, as shown in Fig. 5, although the surface currents are similar due to the assimilation of SSH in the reanalysis process, the cross-track current from reanalysis is quite different from the observation-based absolute geostrophic current. The differences are observed in three aspects. First, the meso-scale eddy CCE2 is not well represented for the vertical structure, as SODA and HYCOM limit the southern part of CCE2 to the upper 200 m, when the current speed is faster than 0.05 m/s. Meanwhile, in SODA and HYCOM, the northern part of the meso-scale eddy (CCE2) has much latitude expansion, and merges the WPPW ~~disturbance (WPD)~~. Second, the undercurrent in the southern portion of the observations differs from those in SODA and HYCOM. The undercurrent in SODA is relatively weak, while HYCOM shows a northward shift of the current core. Finally, for the northern portion, SODA gives a relatively shallow depth for the surface northeastward ~~northeast~~ current, and the corresponding horizontal extent exceeds that of the observations. The locations of surface zero current in SODA and observation are y=170 and 240 km, respectively.

Part of the difference between observation-based absolute geostrophic current and reanalysis current is due to the near-surface Ekman current. The mean surface Ekman speed, which is approximately the difference between surface geostrophic current and in-situ surface current (from surface drifter), is within 0.1 m/s in northern IO (Saj, 2017). Besides, the climatological monthly mean mixed-layer depth in May is roughly 20 m at station 9.5°N and 59.5°E (on CR; Liu et al., 2018). Considering the near-surface Ekman current decays exponentially with depth, therefore, the near-surface Ekman currents in reanalysis datasets are relatively weak to affect the main results as mentioned above.

3.4 Tracers

~~Where the pathways of ASHSW and RSW are concerned, the explanations are still ambiguous. ASHSW and RSW are formed near the northern side of the NWIO; therefore, according to the customary ocean ventilation theory, ASHSW and RSW sink and move southward along the isopycnal layer from the generation zone following the wind-driven current (Luyten et al., 1983).~~ ~~However, in the northern IO, the meridional extent is limited as compared with the other two basins, whether the the ocean ventilation theory is feasible in northern IO is under debate.~~ ~~However, the feasibility of the ocean ventilation theory is still under debate, especially for the northern IO, whose meridional extent is limited compared with the other two basins.~~ ~~For instance, in situ potential vorticity analysis on RSW reveals that the flows generally follow the zonal direction (Beal et al., 2000).~~

Here, the SODA reanalysis supplies compact datasets for passive tracers; therefore, we set some passive tracers along the CR and backtrack their trajectories using the Lagrangian description (section 2.5), and the results are shown in Fig. 6. For the ASHSW, we set the tracers at a depth of 100 m, and the trajectories reveal different pathways on the CR. For better describing the trajectories, we separate the CR to three latitude bands as 2.3-5°N (equatorial band), 5-8°N and 8-9.8°N. ~~For the tropical band (Fig. 6e), the water mainly follows the zonal movement, but the near-equator tracers are from west side and relatively north-side tracers come from east side.~~ In the equatorial band (Fig. 6e), the near-equator tracers come from the west side, which is consistent with the north branch of East African Coastal Current during summer monsoon (Schott and McCreary Jr., 2001; Schott et al., 2009). Meanwhile, for the relatively north-side tracers in equatorial band, the trajectories backtrack to east side, which is probably following a westward current or meso-scale eddy. While for latitudes from 5-8°N (Fig. 6c), the water mainly originates from the northeast side, and the trajectories resemble those of the ventilation theory (Luyten et al., 1983; Qiu and Huang, 1995). The results support ASHSWs are mainly from the Arabian Basin, and the southwestward flow bring the ASHSW into CR. In some occasions, the 100 m depth waters in this latitude section are from the equator, and the pathways show the north branch of East African Coastal Current and the cross-equatorial current around 66°E respectively. Similarly, the pathways start at the east of the Horn of Africa are probably due to the off-coast current at the north of Great Whirl or meso-scale eddies (Chelton et al., 2011; Wang et al., 2019). For latitudes from 8-9.8°N (Fig. 6a), ~~the trajectories look like the flow of the summer Somalia Current (Schott et al., 2009)~~. the trajectories emphasis the north branch of East African

Coastal Current, meanwhile, the water at the north station of CR comes from the northeast side, and one station water shows the cross-equatorial current around 53°E (east of Southern Gyre; Schott et al., 2009).

~~For the RSW in the intermediate-depth layer at 700 m, the trajectories in the tropical band (Fig. 6f) and at latitudes from 5-8°N (Fig. 6d) generally follow the zonal movement (Beal et al., 2000). The tracer movements at latitudes from 8-9.8°N (Fig. 6b) partly agree with those of the ventilation theory, and partly follow the zonal direction (Beal et al., 2000).~~

For the RSW in the intermediate-depth layer at 700 m, the trajectories in the equatorial band (Fig. 6f) show the zonal movement. Most of the trajectories move from the west side, which coincident with the potential vorticity explanation (Beal et al., 2000), that the RSW moves southward along the coast with the help of winter monsoon, and then leave the coast and shift to middle ocean via zonal movement. Other two trajectories come from east side, and one extra trajectory moves from northwest with circular track. Hence, these trajectories display three kinds of pathways. Accordingly, in the 5-8°N band (Fig. 6d), the mainly eastward zonal movements agree with Beal et al. (2000), meanwhile, some westward trajectories resemble the ventilation theory (Luyten et al., 1983; Qiu and Huang, 1995). At last, in the 8-9.8°N (Fig. 6b), new pathway directly from northwest is emerged, and the trajectories support 700 m waters are probably directly from east of the Horn of Africa (or Gulf of Aden) without southward movements along the coast.

4 Discussion

The CTD and XCTD data are precise in reconstructing the three-dimensional oceanic data. Based on theoretical model, three-dimensional ocean interior can be derived using surface information (SSH and sea surface density), where the reliable mean density field is required (Lapeyre and Klein, 2006; Wang et al., 2013; Liu et al., 2014; Yan et al., 2020). In other words, for the operational purpose, the meso-scale eddy coherent structure could be built on known background density field. The Argo-only data are not sufficient to describe the meso-scale eddy in the NWIO, thus could not supply sufficient background density. In the present study, the maximum distance between Argo profiles is 500 km along the CR; however, after adding the shipboard station data, the maximum distance decreases to 100 km, which falls into the eddy-permitting scale. Sufficient sampling produces more reliable vertical structures of temperature, salinity and density.

The most remarkable signal in the upper ocean is the southward extent ~~extension~~ of ASHSW, where the counterpart in the climatology data exists but is weak in the horizontal extent ~~extension~~. It is surprising that the HYCOM reanalysis captures the phenomenon well, while SODA shows some disadvantages. Although both SODA and HYCOM assimilate the Argo data into Oceainc General Circulation Models (OGCMs), the assimilation methods of SODA and HYCOM are considerably different. SODA adopts optimal interpolation (Carton et al., 2018), while HYCOM uses a 3D variational scheme. One advantage of a 3D variational scheme versus optimal interpolation is the conservation of dynamical constraints (Zhu et al., 2006; Yin et al., 2012; Edwards et al., 2015). Therefore, HYCOM probably describes better on the wind-driven circulations, monsoon-induced coastal current and meso-scale eddy movement, which are all related to the southward extent of ASHSW. ~~We speculate that although both SODA and HYCOM assimilate the Argo data into an Oceainc General Circulation Model (OGCM), the methodology of assimilation or the weight between OGCM and in situ observations, is sharply different. We assume the southward extension~~

~~of ASHSW could be simulated by the dynamic core of OGCM, and the phenomenon was not captured in the Argo-only observation, therefore, HYCOM seems more to approach the dynamic model, and SODA weighted more on the Argo-only observations. Additionally, the finer horizontal resolution of HYCOM likely helps HYCOM involve more physically sound mechanics, such as the downwelling of salty water and wind-driven meridional movement.~~

~~Although the geostrophic balance is not universally suitable, it represents a good approximation to the real ocean; therefore, under the circumstance without in situ current observations, the deduced absolute geostrophic current gives alternative results for the ocean current.~~ In the comparative analysis, the state-of-the-art reanalysis is still insufficient to provide good current data. Although similar sea surface dynamic heights are taken into account, the incorrect density field leads to a false vertical structure ~~baroclinic mode~~. It is also noted that the bias is probably further amplified in OGCM and leads to potential unrealistic simulations if these reanalysis data are used in the model for initialization and boundary forcing.

From the theoretical viewpoint, the phase speed of first-, second- and third-mode baroclinic Rossby wave at 6°N in Indian Ocean is roughly 0.6, 0.2 and 0.1 m/s, respectively (Subrahmanyam et al., 2001). The phase speed of WPPW match well with that of the second-mode baroclinic Rossby wave. For the generation mechanics, Subrahmanyam et al. (2001) argued that this kind Rossby wave was probably radiated from coastal trapped Kelvin wave at south-west coast of Indian. Meanwhile, this kind Rossby wave can bring wave energy from south-west coast of Indian to the Somali coast, and feed the Somali Current and Somali eddies. The present study displays the vertical structure of this kind Rossby wave, however, the dynamics of WPPW (and Rossby wave) and the its association with Somali Current and Somali eddies call for further study.

Generally, the hydrothermal plume in CR uplifts from sea bottom to water depth 2500 m (Murton et al., 2006; Wang et al., 2017). Present paper restricts the sectional study to the upper 1050 m (Fig. 4-5). Within this depth, the water is easily affected by surface forcing. However, on the basin-scale wind-driven circulation, the surface wind forcing affects deeper ocean through quasi-geostrophic instability (Rhines and Young, 1982) and meridional overturning circulation. Because present paper concentrates on the CR as well as the cross-ridge current, the upper 1050 m dynamics towards the upper ocean cross-ridge water transport, which is related to the deeper ocean dynamics through pressure adjustment, meanwhile, the activity of meso-scale eddy induces deeper ocean vorticity response (Rhines and Young, 1982), the results provide potential use in the future study of hydrothermal plume event.

5 Conclusions

This paper reports a onetime hydrographic survey on the CR in the NWIO, where the latitudes cover the equatorial ~~tropical~~ (2.3-5°N) and tropical ~~subtropical~~ (5-9.6°N) bands. The station CTD/XCTD sampling plus the Argo floats build the sectional structures of temperature and salinity as well as density. The striking feature is the southern extent ~~extension~~ of ASHSW from northwest of the CR in the upper ocean. Meanwhile, the temperature and density fields display clear ventilation structures. In the intermediate depth, the observations also capture the RSW at a depth near 700 m.

Furthermore, we compute the absolute geostrophic current based on the density profiles and sea surface height ~~we integrate the density field to obtain the absolute geostrophic current~~. The vertical structure of the cross-track current reveals strong signals of meso-scale eddies in the upper ocean and relatively weak northeastward current in the intermediate depth. We also identify a strong westward-propagating planetary wave ~~disturbance~~ at a latitude of 6°N. The longitude and latitude lengths are 7.5° and 1.3° respectively. The corresponding phase speed is 0.2 m/s, and the vertically affected depth is roughly 200 m.

We further evaluate the state-of-the-art reanalysis with the present observations. As a result, because the Argo profiles and satellite SSH are assimilated into the reanalysis datasets, HYCOM and SODA show relatively good qualities for temperature, salinity and density. However, the reanalysis cross-track currents show large discrepancies compared with the absolute geostrophic current. Most importantly, HYCOM and SODA misinterpret some meso-scale eddies in the current field. Over the NWIO, the meso-scale eddies are relatively important but cannot be well described by the Argo-only data source. The present analysis shows more data source for potential data assimilation experiment. ~~The present analysis shows potential data applications for the future, where the meso-scale eddies are relatively important but cannot be well described by the Argo-only data source.~~ The present situation of insufficient sampling prompts more research activity in the NWIO.

To explore the pathways of ASHSW and RSW during the expedition time, we set tracers in SODA dataset at depths of 100 and 700 m, and backtrack their trajectories via three dimensional Lagrangian description. Overall, for the 100 m depth waters, the results reveal the pathways related to the north branch of East African Coastal Current and the flow from northeast side (or Arabian Basin), while for the 700 m depth waters, the trajectories mainly follow the zonal direction from either west and east sides. The results give direct-viewing descriptions and call for further dynamical investigations.

Competing interests. The authors declare that they have no conflict of interest.

Acknowledgements. This work is supported by the China Ocean Mineral Resources Research and Development Association Project (Nos. DY135-S2-1-07 and DY135-E2-1-01) and the National Natural Science Foundation of China (Nos. 41730535 and 41621064). OSTIA SST data were produced by the Meteorological Office of the United Kingdom (http://marine.copernicus.eu/). We are thankful to editor and two anonymous reviewers for their constructive suggestions and comments. WOA data were available in https://www.nodc.noaa.gov/. Daily Argo float data were downloaded from http://www.argodatamgt.org. CCMP wind were provided by Remote Sensing Systems (http://www.remss.com, version 2.0), AVISO SSH data were produced and distributed by the Copernicus Marine and Environment Monitoring Service (CMEMS) (http://www.marine.copernicus.eu), SODA were obtained from http://www.atmos.umd.edu/ ocean/, and HYCOM were downloaded from https://hycom.org/.

References

Atlas, R., Hoffman, R. N., Ardizzone, J., Leidner, S. M., Jusem, J. C., Smith, D. K., and Gombos, D.: A cross-calibrated, multiplatform ocean surface wind velocity product for meteorological and oceanographic applications, Bull. Amer. Meteor. Soc., 92, 157–174, 2011.

Barnes, S. L.: Applications of the Barnes Objective Analysis Scheme. Part I: Effects of Undersampling, Wave Position, and Station Randomness, J. Atmos. Oceanic Technol., 11, 1433–1448, 1994.

Beal, L. M., Ffield, A., and Gordon, A. L.: Spreading of Rea Sea overflow waters in the Indian Ocean, J. Geophys. Res., 105, 8549–8564, 2000.

Beal, L. M., Hormann, V., Lumpkin, R., and Foltz, G.: The Response of the Surface Circulation of the Arabian Sea to Monsoonal Forcing, J. Phys. Oceanogr., 43, 2008–2022, 2013.

Carton, J. A. and Giese, B. S.: A reanalysis of ocean climate using Simple Ocean Data Assimilation (SODA), Monthly Weather Review, 136, 2999–3017, 2008.

Carton, J. A., Chepurin, G. A., and Chen, L. G.: SODA3: A new ocean climate reanalysis, J. Clim., 31, 6967–6983, 2018.

Chelton, D. B. and Schlax, M. G.: Global observations of oceanic Rossby waves, Science, 272, 234–238, 1996.

Chelton, D. B., Schlax, M. G., and M., S. R.: Global observations of nonlinear mesoscale eddies, Progress in Oceanography, 91, 167–216, 2011.

Chen, G. X., Han, W. Q., Li, Y. L., Wang, D. X., and J., M. M.: Seasonal-to-interannual time scale dynamics of the equatorial undercurrent in the Indian Ocean, J. Phys. Oceanogr., 54, 1532–1553, 2015.

Cleveland, W. S. and Grosse, E.: Computational methods for local regression, Stat. Comput., 1, 47–62, 1991.

Donlon, C. J., Martin, M., Stark, J. D., Roberts-Jones, J., E., F., and W., W.: The Operational Sea Surface Temperature and Sea Ice analysis (OSTIA), Remote Sensing of the Environment, 116, 140–158, 2011.

Edwards, C. A., Moore, A. M., Hoteit, I., and Cornuelle, B. D.: Regional ocean data assimilation, Annual Review of Marine Science, 7, 21–42, 2015.

Emery, W. J.: Water Types and Water Masses*, in: Encyclopedia of Ocean Sciences (Second Edition), edited by Steele, J. H., pp. 291 – 299, Academic Press, Oxford, second edition edn., https://doi.org/https://doi.org/10.1016/B978-012374473-9.00108-9, 2001.

Han, W. Q., Vialard, J., McPhaden, M. J., Lee, T., Masumoto, Y., Feng, M., and DE Ruijter, W. P. M.: Indian Ocean decadal variability: A review, Bulletin of the American Meteorological Society, 95, 1679–1703, 2014.

Kumar, S. P. and Prasad, T. G.: Formation and spreading of Arabian Sea high-salinity water mass, J. Geophys. Res. Oceans, 104, 1455–1464, 1999.

Lagerloef, G. S. E., Mitchum, G. T., Lukas, R. B., and Niiler, P. P.: Tropical Pacific near-surface currents estimated from altimeter, wind, and drifter data, J. Geophys. Res.-Oceans, 104, 23 313–23 326, 1999.

Lapeyre, G. and Klein, P.: Dynamics of the Upper Oceanic Layers in Terms of Surface Quasigeostrophy Theory, Journal of Physical Oceanography, 36, 165–176, https://doi.org/10.1175/JPO2840.1, 2006.

Li, Y. L. and Han, W. Q.: Decadal sea level variations in the Indian Ocean investigated with HYCOM: Roles of climate modes, ocean internal variability, and stochastic wind forcing, J. Clim., 28, 9143–9165, 2015.

Liu, L., Peng, S., Wang, J., and Huang, R. X.: Retrieving density and velocity fields of the ocean's interior from surface data, Journal of Geophysical Research: Oceans, 119, 8512–8529, https://doi.org/10.1002/2014JC010221, 2014.

Liu, L. L., Huang, R. X., and Wang, F.: Ventilation of a monsoon-dominated ocean: Subduction and obduction in the North Indian Ocean, J. Geophys. Res. Oceans, 123, 4449–4463, 2018.

Luyten, J. L., Pedlosky, J., and Stommel, H. M.: The ventilated thermocline, J. Phys. Oceanogr., 13, 292–309, 1983.

McCreary, J. P.: Modeling equatorial ocean circulation, Annual Review of Fluid Mechanics, 17, 359–409, 1985.

Murton, B. J., Baker, W. T., Sands, C. M., and German, C. R.: Detection of an unusually large hydrothermal event plume above the slow-spreading Carlsberg Ridge: NW Indian Ocean, Geophys. Res. Lett., 33, L10608, 2006.

Prasad, T. G., Ikeda, M., and Kumar, S. P.: Seasonal spreading of the Persian Gulf Water mass in the Arabian Sea, J. Geophys. Res. Oceans, 106, 17 059–17 071, 2001.

Qiu, B. and Huang, R. X.: Ventilation of the North Atlantic and North Pacific: Subduction versus obduction, J. Phys. Oceanogr., 25, 2374–2390, 1995.

Rhines, P. B.: Waves and turbulence on a beta-plane, J. Fluid Mech., 69, 417–443, 1975.

Rhines, P. B. and Young, W. R.: Homogenization of potential vorticity in planetary gyres, J. Fluid Mech., 122, 347–367, 1982.

Riser, S. C., Freeland, H. J., Roemmich, D., Wijffels, S., Troisi, A., Belbeoch, M., Gilbert, D., Xu, J., Pouliquen, S., Thresher, A., Le Traon, P.-Y., Maze, G., Klein, B., Ravichandran, M., Grant, F., Poulain, P.-M., Suga, T., Lim, B., Sterl, A., Sutton, P., Mork, K.-A., Velez-Belchi, P. J., Ansorge, I., King, B., Turton, J., Baringer, M., and Jayne, S. R.: Fifteen years of ocean observations with the global Argo array, Nature Climate Change, 6, 145–153, 2016.

Saj, R. P.: Surface velocity estimates of the North Indian Ocean from satellite gravity and altimeter missions, International Journal of Remote Sensing, 38, 296–313, 2017.

Saji, N. H., Goswami, B. N., Vinayachandran, P. N., and Yamagata, T.: A dipole mode in the tropical Indian Ocean, Nature, 401, 360–363, 1999.

Schott, F. A. and McCreary Jr., J. P.: The monsoon circulation of the Indian Ocean, Progress in Oceanography, 51, 1–123, 2001.

Schott, F. A., Xie, S. P., and McCreary Jr., J. P.: Indian Ocean circulation and climate variability, Reviews of Geophysics, 47, RG1002, 2009.

Sharma, G. S., Gouveia, A. D., and Satyendranath, S.: Incursion of the Pacific Ocean water into the Indian Ocean, Proc. Indian Acad. Sci., 87A, 29–45, 1978.

Subrahmanyam, B., Robinson, I. S., Blundell, J. R., and Challenor, P. G.: Indian ocean Rossby waves observed in TOPEX/POSEIDON altimeter data and in model simulations, International Journal of Remote Sensing, pp. 141–167, 2001.

Talley, L. D., Pickard, G. L., Emery, W. J., and S., J. H.: Descriptive physical oceanography: An introduction, Elsevier, Burlingham, 6 edn., 2011.

Vecchi, G. A., Xie, S. P., and Fischer, A. S.: Ocean-atmosphere covariability in the Western Arabian Sea, Journal of Climate, 17, 1213–1224, 2004.

Vitale, S. S., DiMarco, S. F., Seidel, H. F., and Wang, Z. K.: Circulation analysis in the northwest Indian Ocean using ARGO floats and surface drifter observations, and SODA reanalysis output, Dynamics of Atmospheres and Oceans, 78, 57–70, 2017.

Wang, J., Flierl, G. R., LaCasce, J. H., McClean, J. L., and Mahadevan, A.: Reconstructing the Ocean's Interior from Surface Data, Journal of Physical Oceanography, 43, 1611–1626, https://doi.org/10.1175/JPO-D-12-0204.1, 2013.

Wang, S., Zhu, W. J., Ma, J., Ji, J. L., Yang, J. S., and Dong, C. M.: Variability of the Great Whirl and its impacts on atmospheric processes, Remote Sensing, 11, 322, 2019.

Wang, Y. J., Han, X. Q., Petersen, S., Frische, M., Qiu, Z. Y., Li, H. M., Li, H. L., Wu, Z. C., and Cui, R. Y.: Mineralogy and trace element geochemistry of sulfide minerals from the Wocan Hydrothermal Field on the slow-spreading Carlsberg Ridge Indian Ocean, Ore Geology Reviews, 84, 1–19, 2017.

Webster, P. J., Moore, A. M., Loschnigg, J. P., and Leben, R. R.: Coupled ocean-atmosphere dynamics in the Indian Ocean during 1997-98, Nature, 401, 356–360, 1999.

Xie, S. P., Annamalai, H., Schott, F. A., and McCreary Jr., J. P.: Structure and mechanisms of south Indian Ocean climate variability, J Clim, 15, 864–878, 2002.

Yan, H., Wang, H., Zhang, R., Chen, J., Bao, S., and Wang, G.: A Dynamical-Statistical Approach to Retrieve the Ocean Interior Structure From Surface Data: SQG-mEOF-R, Journal of Geophysical Research: Oceans, 125, e2019JC015 840, https://doi.org/10.1029/2019JC015840, 2020.

Yang, G., He, H. L., Wang, Y., Han, X. Q., and Wang, Y. J.: Evaluating a satellite-based sea surface temperature by shipboard survey in the Northwest Indian Ocean, Acta Oceanologica Sinica, 35, 52–58, 2016.

Yin, X. Q., Qiao, F. L., Yang, Y. Z., Xia, C. S., and Chen, X. Y.: Argo data assimilation in ocean general circulation model of Northwest Pacific Ocean, Ocean Dynamics, 62, 1059–1071, 2012.

You, Y.: Intermediate water circulation and ventilation of the Indian Ocean derived from water-mass contributions, Journal of Marine Research, 56, 1029–1067, https://doi.org/doi:10.1357/002224098765173455, 1998.

Zhu, J., Zhou, G. Q., X., Y. C., Fu, W. W., and You, X. B.: A three-dimensional variational ocean data assimilation system: Scheme and preliminary results, Science in China Series D: Earth Sciences, 49, 1212–1222, 2006.

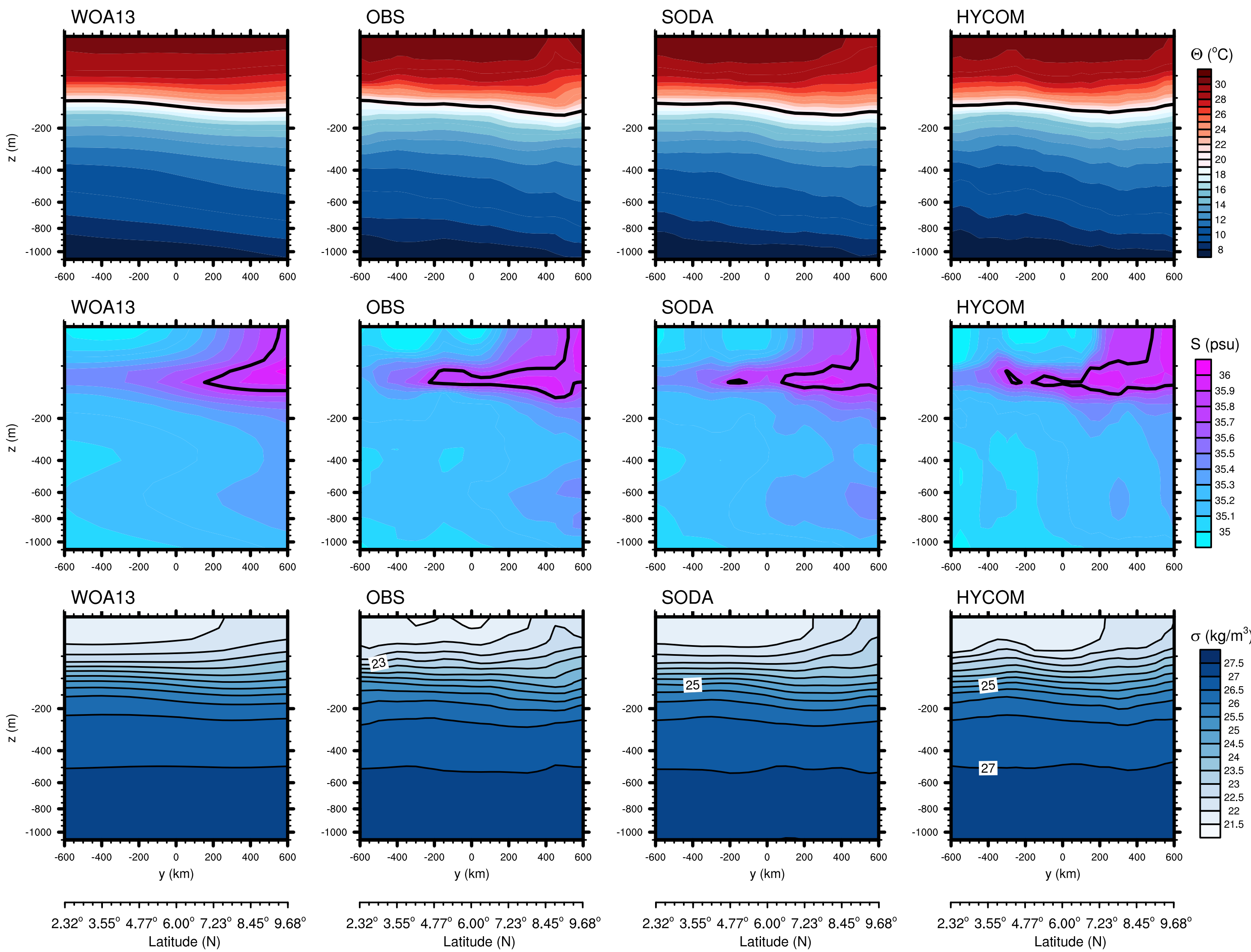

Figure 4. Sectional profiles of potential temperature (upper panels), salinity (middle panels) and potential density (lower panels). The data sources cover the WOA climatology (WOA13, version 2.0/A5B2), the present observations, and two reanalysis datasets, SODA and HYCOM. The isothermal lines of 20^{o}C are presented at potential temperatures, and the iso-salinity lines of 35.8 psu are highlighted in the salinity fields.

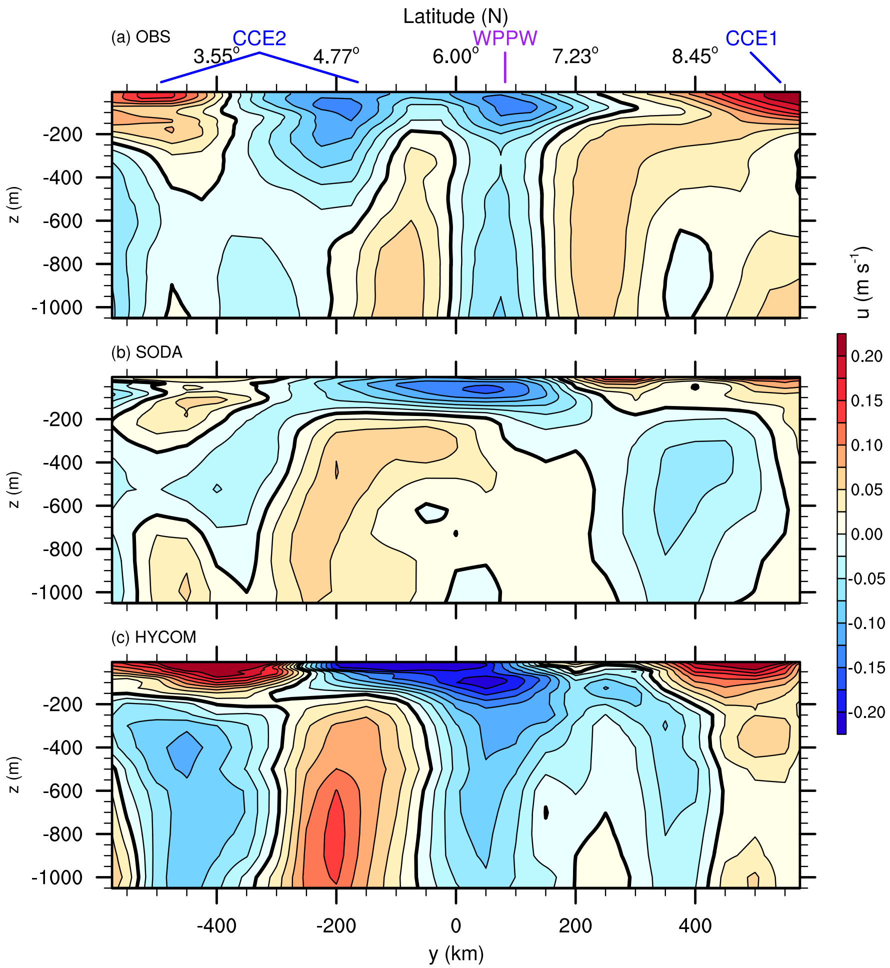

Figure 5. Sectional cross-track current: (a) absolute geostrophic current; (b and c) currents in SODA and HYCOM reanalysis, respectively. Northeastward current is positive. Thick black lines are the zero contours.

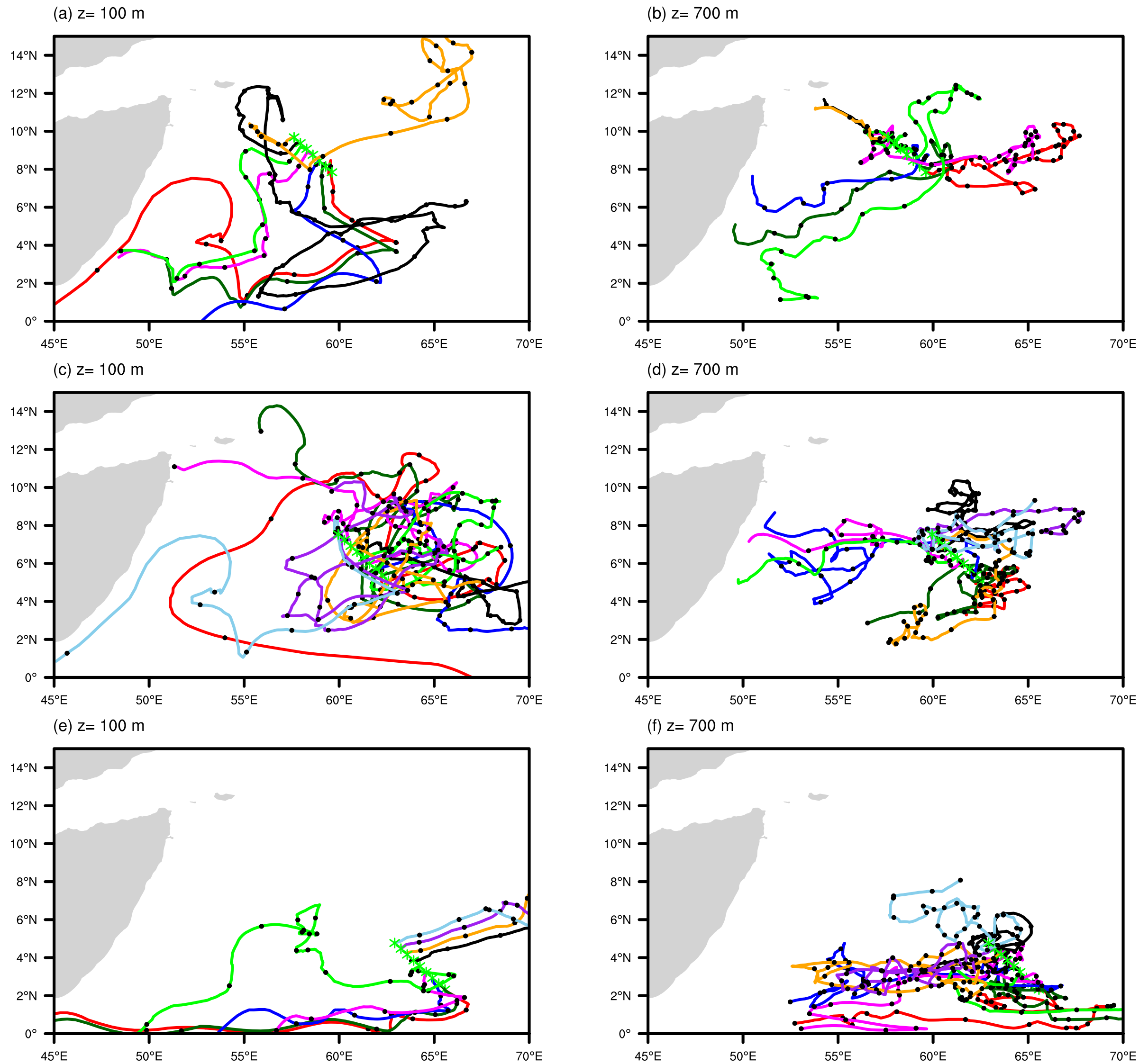

Figure 6. Passive tracers using SODA reanalysis. ~~The tracers are set along the CR on May 15, 2012 (denoted by green asterisks), and then backward integrated to Jan. 1, 2010.~~ The time interval is one month, as denoted by the black dots. (a-b) 8-9.8°N; (c-d) 5-8°N; (e-f) 2-5°N.

Response to editor

Thank-you for your revised manuscript. Unfortunately I think it is not ready to go back to reviewers, which will be necessary before publication. The most serious comments are: lack of clear objectives beyond describing the observations, a point made by both reviewers ? this should be at the end of the Introduction; the manuscript (pages 3, 4) does not answer reviewer 2 point 2 wanting better explanation of methods; you do not explain what you mean by WPD or describe it; there is description but very little dynamical interpretation which was wanted by the reviewers.

Response: Thanks to editor for reading throughout the manuscript again and giving inspiring suggestions. We made revisions mainly including:

(1) Clarifying the main objective of present paper at the end of Introduction:

"First, hydrographic survey takes a snapshot on the water mass, and gives an evidence on the activity of water mass. Second, the observation probably captures the vertical structure of meso-scale eddy or planetary wave. Third, the results could be used to evaluate the widely-used oceanic reanalysis. "

(2) As response to better explanation of the method, we did not calibrate the instrumental readings. XCTD observations were compared to both ship CTD and Argo observation. However, every XCTD and Argo has individual sensor, we did not impose calibration on these datasets. In the revised manuscript, we stated as:

"Differences among CTD, XCTD and Argo are not negligible. However, because the distances between two stations in comparisons are relatively large, and the biases of XCTD and Argo are different for instruments, we does not perform instrument calibration."

In addition, Argo data are not need further calibrated, the official site already made data quality control.

(3) On the dynamical interpretation of WPD (changed to west-propagating planetery wave, WPPW), we add some discussion at Section Discussion, as

"From the theoretical viewpoint, the phase speed of first-, second- and third-mode baroclinic Rossby wave at 6°N in Indian Ocean is roughly 0.6, 0.2 and 0.1 m/s, respectively (Subrahmanyam et al., 2001). The phase speed of WPPW match well with that of the second-mode baroclinic Rossby wave. For the generation mechanics, Subrahmanyam et al., (2001) argued that this kind Rossby wave was probably radiated from coastal trapped Kelvin wave at southwest coast of Indian. Meanwhile, this kind Rossby wave can bring wave energy from southwest coast of Indian to the Somali coast, and feed the Somali Current and Somali eddies. The present study displays the vertical structure of this kind Rossby wave, however, the dynamics of WPPW (and Rossby wave) and the its association with Somali Current and Somali eddies call for further study. "

Here follow detailed comments intended to improve clarity. Page and line numbers refer to the "clean" version of the revised manuscript.

Page 1
Line 15. ". . the monsoon is strong enough to change . ."
Response: Corrected.

Line 16. Omit "which"
Response: Corrected.

Line 17. ". . into a meridional current. . "
Response: Corrected

Line 22. ". . main water masses . . are understood . ." is not very sensible. It might mean that we understand how these water masses are formed but you do not say anything about that. Perhaps ". . main water masses . . have been described . ."
Response: Corrected. "understood" was replaced by "described".

Page 2
lines 4-5. I do not understand "feasibility of the ocean ventilation theory is still unknown for the northern IO?. Maybe "feasibility" → "applicability" In any case you should explain why there is this uncertainty ? why should the limited (but still large) meridional extent of the Indian Ocean negate ventilation theory?
Response: "applicability of the ocean ventilation theory is still unknown for the northern IO, because the surface wind reverse directions under the influence of winter monsoon (Liu et al., 2018). Meanwhile, the limited meridional extent of Indian Ocean omits the polar-to-subpolar front, which help forms intermediate water in Pacific Ocean and Atlantic Ocean (You et al., 1998)."

Line 5. Be explicit: what are the "other two basins"?
Response: Corrected.

Line 6. So there is a contrast between the two ideas. Which corresponds with observations? Or is it an aim of the manuscript to answer this through observations?
Response: Yes. The study of Beal et al. (2000) is based on observations. We added: "How the water mass moves is worthy further investigation."

Line 9. "close to the tropic?"? unclear, use your revised definitions.
Response: Corrected.

Lines 11-12. " Rossby wave, . . . and west-propagating disturbance". What is the difference? Or definition of west-propagating disturbance? Rossby waves propagate westwards.
Response: We changed "west-propagating disturbance" to "west-propagating planetary wave". The old version is
"The planetary waves at-least include Rossby wave, Kelvin wave and west-propagating disturbance (Rhines, 1975; McCreary, 1985). Specifically, the vertical structure of the west-

propagating disturbance needs further investigation in NWIO (Maximenko et al., 2005)."
The new version is
"Besides, the planetary waves at-least include Rossby and Kelvin waves (Rhines, 1975; McCreary, 1985). Satellite-retrieved sea surface height are commonly used to detect the planetary waves (Chelton and Schlax, 1996), however, the internal dynamics of planetary wave is not sufficiently addressed. The phase speed of west-propagating planetary wave (WPPW) is used to match the theoretical Rossby wave, nonetheless, the vertical structure of WPPW calls for vertical profiling observation (Subrahmanyam et al., 2001)."

Lines 15-16. "interdisciplinary survey" (spellings).
Response: Corrected.

Line 16. "and the CTD and XCTD station data have not yet been explored." You cannot say this because you use them in this manuscript. You could say (earlier, if true) that previous CTD and XCTD data are lacking.
Response: We deleted "and the CTD and XCTD station data have not yet been explored".

Lines 17-22. These aims are still very unclear and mostly not attempted in the manuscript. Line 19. "this analysis provides a reference to the basic energy theory" is especially unclear.
Response: We modified the statement as
"First, hydrographic survey takes a snapshot on the water mass, and gives an evidence on the activity of water mass. Second, the observation probably captures the vertical structure of meso-scale eddy or planetary wave. Third, the results could be used to evaluate the widely-used oceanic reanalysis. "

Page 3
line 4. 47.17km is quite a large separation, comparable with an internal deformation radius (eddy or internal wave scale).
Line 9. 79.97 km ? same comment. How do you use these comparisons (XCTD versus CTD; XCTD versus Argo) to calibrate* or estimate uncertainties in which instrument readings? *According to your response to reviewer 2 you did not calibrate the readings but the manuscript needs to be explicit about this.
Response: We added
"Differences among CTD, XCTD and Argo are not negligible. However, because the distances between two stations in comparisons are relatively large, and the biases of XCTD and Argo are different for instruments, we does not perform instrument calibration."

Page 4 bottom lines. "We later use objective analysis method and low-pass filter to reduce the differences among CTD, XCTD and Argo." is very unclear. Differences between the values from various measurement methods are unalterable facts and cannot be reduced.
Response: The sentence is modified as
"We later use objective analysis method and low-pass filter to smooth the data among CTD,

XCTD and Argo."

Page 5

Line 8. "with a uniform 100 km interval in the y-coordinate" is unclear. Does this mean data located over a y-range 100 km are all merged? 100 km seems a very coarse grid spacing. Some features in figure 2 have scales smaller than this.

Response: The interval distance is 50 km actually. We sorry for the mistake.

"The data are then projected into the standard CR section with a uniform 100 km interval in the y-coordinate"

was changed to

"The data are then projected into the standard CR section (y-coordinate), and the corresponding grid interval is 50 km."

Lines 9-14. What about time? Are all data from the month merged to one description? If so, you cannot refer to west-propagating disturbance because you cannot "see" propagation.

Response: Yes. All data from the month merged to one description. We find the west-propagating disturbance from longitude-time plot of SSH data. We changed the "west-propagating disturbance (WPD)" to "west-propagating planetary wave (WPPW)" in the revised manuscript.

Page 6

Line 5. ". . observations."

Response: Corrected.

Line 12. Omit "interval of"

Response: Corrected.

Line 16. ". . starts . . ends . ."

Response: Corrected.

Lines 17-18. You can omit "which is preferentially defined as the later stage of monsoon transition,"

Response: Corrected.

Line 19-20. "Positive wind curl . . . induces sufficient coastal upwelling". Maybe. But the upwelling is strongest at the coast which suggests that the wind stress at the coast is the main cause; it drives off-coast Ekman water transport. In fact positive wind (stress) curl drives upwelling, not exactly off-coast transport.

Response: We revised the sentence as "Positive wind curl along the Somalia coast and Yemen induces sufficient coastal upwelling, which brings lower-layer cold water upward and cools the sea surface (Fig. 2b)."

Line 22. You can omit "dominant".
Response: Corrected.

Lines 23-24. Better ". . annual mean, and forces downwelling. The basin-scale . ."
Response: Corrected.

Line 24. "front"? The changes are over 100s km, is this scale small enough to be called a "front"?
Response: We replaced "front" by "contour (30°C)", and deleted the following "where SST exceeds 30°C".

Page 7,
bottom lines. ". . propagating . . (WPD). . ." Your response refers to Maximenko et al. (2005). You should cite it here. How do you tell that the WPD is propagating? I agree that the westward current at 6N is exceptional for its zonal extent, but not for its magnitude: there are several other places in figure 2c where the arrows indicate currents of order 0.4 m/s.
Response: The description in "Section 3.3 Cross-track current" was moved here, as
"Furthermore, we investigated the longitude-time plot of the surface zonal current at 6°N latitude (surface geostrophic current from SSH; results are not shown here), the WPD is observed to start at 69°E on day 102, the surface current propagates westward with a phase speed of 0.2 m s^{-1} and arrives at 60°E on day 155."
Meanwhile, we changed
"which refers to not only the magnitude (-0.38 m/s for the zonal current) but also the zonal extent (7.5° in longitude), although its meridional extent is relatively narrow (1.3° in latitude)."
into
"which refers to the zonal extent (7.5° in longitude), while the meridional extent is relatively narrow (1.3° in latitude). The magnitude of zonal current is -0.38 m/s."

Page 8
Lines 15-16. "some isothermal lines rise to the surface on the northern side and show a clear ventilation structure". "some" = "one" and this is not sufficient to show the temperature range of what rises to the surface. This might all be mixed layer by the definition in your response. Therefore not "clear".
Response: We replaced the "some isothermal lines" into "isothermal line of 30°C", and we added the line-labels on temperature and salinity fields in Figure 4.

Line 25. "on the activities" → "for the distributions"
Response: Corrected.

Lines 26, 27. ". . in both the snapshot and climatology." And in SODA and HYCOM?
Response: The density fields of SODA and HYCOM were later described in the following second paragraph.

Lines 27-30. How are these sentences related to each other? What about 21.9 or 22.1 kg/m3 outcrops?
Response: We added a sentence to explain the relationship, as"and the results suggest that the ventilation is induced by surface wind". Because we use 22 kg/m3 as an example, we do not take other isopycnal for discussion.

Line 33. ". . y=400 km where it crops out. . ." What does "it" refer to? I think cooler subsurface water but this needs to be explicit because it was not mentioned immediately before.
Response: "it" is changed to "the isothermal line of 30°C".

Line 33. Not "steeply"; even in oceanography, 50 m / 200 km is not steep.
Response: We deleted "steeply".

Line 34. The largest slope is at different values of y in OBS compared with SODA and HYCOM, so not "reproduced".
Response: We changed "reproduced" into "recognizable".

Page 9 figure 3. The separation of these profiles $\sim$ 1.9 °N is much more than the 100 km "grid" of section 2.2.
Response: We displayed more data in the figure as revision.

Page 10
Line 17. "observed to start at 69°E on day 102, propagate westward with a phase speed of 0.2 m s $^{-1}$ and arrive at 60oE on day 155." Presumably this is from SSH from altimetry. This may explain how you can "see" propagation (WPD). But what exactly is propagating?
Response: The phase of surface current is propagating.
"the WPD are observed to start at 69°E on day 102, propagate westward with a phase speed of 0.2 m s $^{-1}$ and arrive at 60°E on day 155."
was changed to
"the WPD is observed to start at 69°E on day 102, the surface current propagates westward with a phase speed of 0.2 m s $^{-1}$ and arrives at 60°E on day 155."

Line 32 to page 11 line 1. 0.1 m/s is not "relatively weak" compared with typical currents in figure 5.
Response: Accordingly, we added "Considering the near-surface Ekman current decays exponentially with depth, ..."

Page 11.
Line 13. "which agrees with the ASHSW definition". I don't think a movement can agree with a definition. Please rewrite the lines 12-14 sentence.
Response: We deleted "which agrees with the ASHSW definition".

Line 30. "The CTD and XCTD data are precise in reconstructing the three-dimensional oceanic

data." But in section 2.2. you said that "The data are then projected into the standard CR section? which is only 2-D. And indeed the stations in figure 1 have very little x-extent.
Response: In the revised version, we stated as
"The CTD and XCTD data are precise in reconstructing the three-dimensional oceanic data. Based on theoretical model, three-dimensional ocean interior can be derived using surface information (SSH and sea surface density), where the reliable mean density field is required (Lapeyre and Klein, 2006; Wang et al., 2013; Liu et al., 2014; Yan et al., 2020). In other words, for the operational purpose, the meso-scale eddy coherent structure could be built on known background density field. The Argo-only data are not sufficient to describe the meso-scale eddy in the NWIO, thus could not supply sufficient background density."

Page 12
Lines 3, 4. "extension" → "extent"? And many other places?
Response: Corrected.

Line 7. "3D variation" → "a 3D variational" (twice) ?
Response: Corrected.

Lines 7, 8. "optimum" → "optimal"?
Response: Corrected.

Line 8. "constraints" (spelling).
Response: Corrected.

Line 9. Omit "on"
Response: Corrected.

Line 12. "mode" → "structure"
Response: Corrected.

Line 15. "in" → "to". "easy" → "easily"
Response: Corrected.

Lines 17-20. This is very unclear. How can the "present . . results", down to 1050 m only, be useful in a study of a hydrothermal plume event below 2500 m?
Response: We added an explanation, as
"the upper 1050 m dynamics towards the upper ocean cross-ridge water transport, which is related to the deeper ocean dynamics through pressure adjustment, meanwhile, the activity of meso-scale eddy induces deeper ocean vorticity response (Rhines and Young, 1982),"

Page 13 line 2. "HYCOM and SODA misinterpret some meso-scale eddies". I did not see where you state the time-period of the HYCOM and SODA reanalyses. Eddies move! Why should we expect HYCOM and SODA to match the May 2012 observations?
Response: We added the time period of HYCOM and SODA reanalysis in "Section 2.4 Re-

analysis data description". HYCOM and SODA assimilate the sea surface height data, which include the signal of meso-scale eddy. In some occasion, HYCOM and SODA are used to describe the vertical structure of meso-scale eddy (Liu et al., 2014).

Liu, L., Peng, S., Wang, J., and Huang, R. X. (2014), Retrieving density and velocity fields of the ocean's interior from surface data, J. Geophys. Res. Oceans, 119, 8512? 8529, doi:10.1002/2014JC010221.

Page 17, figure 4 caption lines 2-3. ".. . 20^o are highlighted in the potential temperatures . ."
Response: Corrected.

Hydrographic survey over the Carlsberg Ridge in May 2012

Hailun He[1], Yuan Wang[2], Xiqiu Han[2], Yanzhou Wei[1], Pengfei Lin[3], Zhongyan Qiu[2], and Yejian Wang[2]

[1]State Key Laboratory of Satellite Ocean Environment Dynamics, Second Institute of Oceanography, Ministry of Natural Resources, Hangzhou 310012, China

[2]Key Laboratory of Submarine Geosciences, Second Institute of Oceanography, Ministry of Natural Resources, Hangzhou 310012, China

[3]State Key Laboratory of Numerical Modeling for Atmospheric Sciences and Geophysical Fluid Dynamics, Institute of Atmospheric Physics, Chinese Academy of Sciences, Beijing 100029, China

Correspondence: Hailun He (hehailun@sio.org.cn); Xiqiu Han (xqhan@sio.org.cn)

Abstract. In May 2012, we conducted a hydrographic survey over the Carlsberg Ridge in the northwest Indian Ocean. In this paper, we use these station data, in combination with some free-floating Argo profiles, to obtain the sectional temperature and salinity fields, and subsequently, the hydrographic characteristics are comprehensively analyzed. Through the basic T-S diagram, three salty water masses, Arabian Sea High-Salinity Water, Persian Gulf Water, and Red Sea Water, are identified. The sectional data show a clear ventilation structure associated with Arabian Sea High-Salinity Water. The 35.8 psu salty water sinks at 6.9°N and extends southward to 4.4°N at depths around the thermocline, where the thermocline depth is in the range of 100 to 150 m. This salty thermocline extends much further south than the climatology indicates. Furthermore, the temperature and salinity data are used to compute the absolute geostrophic current over the specific section, and the results show meso-scale eddy vertical structure different from some widely used oceanic reanalysis data. We also find a west-propagating planetary wave~~disturbance~~ at 6°N, and the related features are described in terms of phase speed, horizontal and vertical structures.

1 Introduction

The northwest Indian Ocean (NWIO) is unique compared with the other two basin-scale oceans (Pacific and Atlantic Oceans) because the dominant characteristics are monsoon driven (Schott and McCreary Jr., 2001; Schott et al., 2009). The seasonal monsoon forces the coastal current back and forth and generates the Somalia Current, which is always marked as the strongest current in the real ocean (as strong as 3.5 m s^{-1}). Moreover, the monsoon is strong enough to ~~so strong to~~ change the pattern of basin-scale circulation. The monsoon builds up a dominant meridional current in the NWIO, ~~which~~ changing the form of the customary zonal current (as in the Pacific and Atlantic Oceans) into a ~~the~~ meridional current. NWIO is also famous for its role in the so-called Indian Ocean Dipole (IOD; Saji et al., 1999; Webster et al., 1999; Han et al., 2014; Chen et al., 2015), which represents the zonal gradient of sea surface temperature (SST) in the Indian Ocean (IO). As a basin-wide signal, the IOD is closely related to the IO-adjacent climate (Li and Han, 2015). Some studies also emphasized the distinct meso- and submeso-scale air-sea interactions in the NWIO (Vecchi et al., 2004).

To date, the main water masses in the IO and NWIO have been described ~~are understood~~ by the scientific community (Sharma et al., 1978; Kumar and Prasad, 1999; Emery, 2001; Talley et al., 2011). For instance, three water masses were defined in NWIO as Arabian Sea High-Salinity Water (ASHSW), Persian Gulf Water (PGW) and Red Sea Water (RSW). Regarding the pathways of these water masses, the mechanics are not clear. RSW is formed near the northern side of the NWIO; therefore, according to the customary ocean ventilation theory, RSW sinks and moves southward along the isopycnal layer from the generation zone following the wind-driven current (Luyten et al., 1983). However, the applicability of the ocean ventilation theory is still unknown for the northern IO, because the surface wind reverses direction under the influence of winter monsoon (Liu et al., 2018). Meanwhile, the limited meridional extent of IO omits the polar-to-subpolar front, which helps forming intermediate water in Pacific and Atlantic Oceans (You, 1998). ~~However, the feasibility of the ocean ventilation theory is still unknown for the northern IO, whose meridional extent is limited compared with Pacific and Atlantic Oceans the other two basins.~~ In contrast, in situ potential vorticity analysis on RSW reveals that the flows generally follow the zonal direction (Beal et al., 2000). How the water mass moves is worthy further investigation.

On the other hand, the meso-scale eddies and planetary waves are not sufficiently observed in NWIO. The historical and present Research Moored Array for African-Asian-Australian Monsoon Analysis and Prediction (RAMA) observation arrays are close to the equator~~tropic~~ and omit the NWIO. In situ observations in the NWIO mainly depend on Array for Real-time Geostrophic Oceanography (Argo; Riser et al., 2016; Vitale et al., 2017). However, as we show later, the number of Argo floats is still too sparse to represent the meso-scale eddy field in the NWIO. Besides, the planetary waves at-least include Rossby and Kelvin waves (Rhines, 1975; McCreary, 1985). Satellite-retrieved sea surface height are commonly used to detect the planetary waves (Chelton and Schlax, 1996), however, the internal dynamics of planetary wave is not sufficiently addressed. The phase speed of west-propagating planetary wave (WPPW) is used to match the theoretical Rossby wave, nonetheless, the vertical structure of WPPW calls for vertical profiling observation (Subrahmanyam et al., 2001). ~~The planetary waves at-least include Rossby wave, Kelvin wave and west-propagating disturbance (Rhines, 1975; McCreary, 1985). Specifically, the vertical structure of the west-propagating disturbance needs further investigation in NWIO (Maximenko et al., 2005).~~

The present circumstance stimulates our effort to find more observational resources. The Carlsberg Ridge (CR) is a typical slow-spreading ridge and lies along the northwest-southeast direction in the NWIO. Recently, we conducted an interdiscriplinary ~~interdiscripline~~ survery on CR (Yang et al., 2016; Wang et al., 2017)~~, and the CTD and XCTD station data have not yet been explored.~~ , and the hydrographic ~~Hydrographic~~ analysis of CR is necessary for at least three reasons. First, hydrographic survey takes a snapshot on the water mass, and gives an evidence on the activity of water mass. Second, the observation probably captures the vertical structure of meso-scale eddy or planetary wave. Third, the results could be used to evaluate the widely-used oceanic reanalysis. ~~First, such analysis helps us to define regional ocean circulation and regional multiscale air-sea interactions. Second, the analysis supplies basic environmental parameters to determine the movements of sporadic hydrothermal activity. Third, this analysis provides a reference to the basic energy theory of ocean circulation (Huang, 1999)~~ The trajectory of Argo float are not manually controlled; however, ship surveys could cover specified sections and have a clearer objective. Hence, this paper aims to analyze hydrographic information by combining both CR expedition and Argo floats.

2 Data and methods

2.1 In situ data description

The data for our study were collected during the Chinese cruise DY125-24 (May 2012) by the Chinese research vessel "LISIGUANG". Hydrographic observations were conducted in the region of the CR ~~Carlsberg Ridge~~. The vertical profiles of temperature, conductivity and pressure were obtained by a calibrated SBE-19plus CTD and some expendable CTD (XCTD). The station information is shown in Fig. 1 and Table 1. All stations were mainly located along the CR section and therefore defined the regional along-section (y) and cross-section (x) coordinates. The maximum measurement depths of XCTD and Argo are 1050 and 2000 m, and therefore we limited our analysis to depth 2000 m. According to Talley et al. (2011) and Emery (2001), upper 2000 m depth covers the upper ocean (defined as 0-500 m) and the intermediate-depth ocean (defined as 500-2000 m).

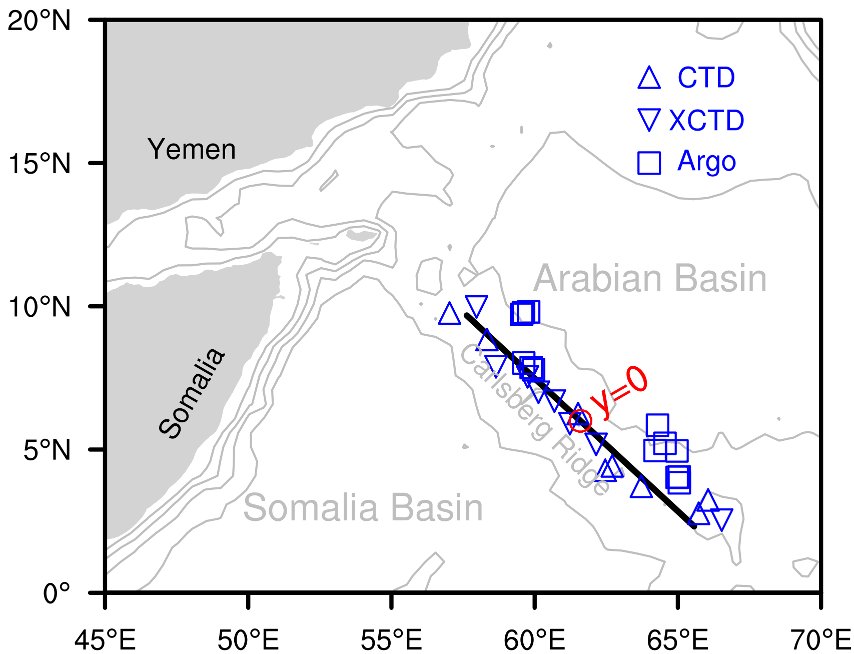

Figure 1. CTD/XCTD stations of the DY125-24 survey and the simultaneous Argo profiles around the CR. The CR defines local coordinates in which the x-coordinate is cross-track and the y-coordinate along-track, the corresponding origin point is selected as (61.6°E, 6.0°N), and the isobaths of -4000, -3000, -2000 and -1000 m are presented.

Regarding data quality, an intercomparison between XCTD and CTD measurement was implemented in the southern tropical Indian Ocean. The XCTD station involved was located at 73.8°E and 1.7°S at 14:23 on May 4 (Coordinated Universal Time), and the counterpart CTD station was located at 73.5°E and 1.4°S a half-hour later (14:58 on May 4; distance with the XCTD station as 47.17 km). The mean differences in the recorded in situ temperature (salinity) were 0.425°C (0.058 psu) in the upper ocean and 0.051°C (0.053 psu) in the intermediate-depth ocean.

Table 1. Information on CTD/XCTD stations and Argo floats.

Type	Station/Float	Latitude	Longitude	Time (month/day hour)
XCTD	S09CTD08	2.3°N	66.3°E	05/06 07
XCTD	S16CTD13	5.1°N	62.1°E	05/14 16
XCTD	S19CTD15	6.4°N	60.4°E	05/16 13
XCTD	S20CTD16	7.3°N	59.5°E	05/16 19
XCTD	S23CTD19	7.0°N	60.1°E	05/20 14
XCTD	S25CTD21	9.6°N	57.6°E	05/23 04
XCTD	S26CTD22	5.5°N	61.1°E	05/26 20
CTD	S10CTD09	3.1°N	66.0°E	05/07 05
CTD	S12CTD10	2.5°N	65.4°E	05/09 12
CTD	S14CTD11	4.2°N	62.3°E	05/11 17
CTD	S15CTD12	4.3°N	62.4°E	05/13 21
CTD	S17CTD14	6.2°N	61.3°E	05/15 08
CTD	S21CTD17	8.5°N	58.2°E	05/17 05
CTD	S22CTD18	9.5°N	57.0°E	05/18 07
CTD	S28CTD24	3.4°N	63.4°E	06/01 04
Argo	2901847	4.0°N	65.0°E	05/03 02
Argo	2901848	5.8°N	64.3°E	05/07 13
Argo	2900877	8.0°N	59.6°E	05/07 09
Argo	2901096	5.0°N	64.2°E	05/08 19
Argo	2901888	9.7°N	59.5°E	05/08 01
Argo	2901847	4.0°N	65.0°E	05/12 20
Argo	2901888	9.8°N	59.6°E	05/17 23
Argo	2900877	7.9°N	59.9°E	05/17 09
Argo	2901096	5.2°N	64.6°E	05/18 19
Argo	2901847	3.8°N	65.1°E	05/22 16
Argo	2900877	7.8°N	60.0°E	05/27 09
Argo	2901096	5.0°N	65.0°E	05/28 18
Argo	2901888	9.8°N	59.8°E	05/28 01

In our postprocessing, 13 simultaneous Argo profiles were found within a 200 km radius of the study region (Fig. 2 and Table 1). The Argo float is free-floating without regular calibration; therefore, quantifying the uncertainty ~~bias~~ of Argo is relatively important before using the data. Fortunately, an Argo float drifted (2900877) around an XCTD station (S20CTD16; Table 1;

distance with the Argo float as 79.97 km), and the two measurements occurred on May 17 and May 16, respectively. Then, we compared the XCTD with the Argo profile, and the mean differences in the in situ temperature (salinity) were 0.076°C (0.144 psu) in the upper ocean and 0.374°C (0.171 psu) in the intermediate-depth ocean. It is also noted that the differences for temperature and salinity in the intermediate depth ocean are much larger than those in the upper ocean, which is probably due to the oceanic internal high-wavenumber signals between two stations. Differences among CTD, XCTD and Argo are not negligible. However, because the distances between two stations in comparisons are relatively large, and the biases of XCTD and Argo are different for instruments, we does not perform instrument calibration. We later use objective analysis method and low-pass filter to smooth the data among CTD, XCTD and Argo. ~~We later use objective analysis method and low-pass filter to reduce the differences among CTD, XCTD and Argo.~~

2.2 In situ data processing

All the data from several sources need to be processed to same levels because of the different sampling rates; i.e., the vertical resolutions of CTD, XCTD and Argo are 0.1, 0.1, and 2.0 m, respectively. In the first step of data postprocessing, the coarse data are moving-averaged into a uniform vertical grid with a 5 m interval starting from 5 m below the surface. Here 5 m vertical resolution is sufficient for describing vertical structure of mixed-layer and water masses. Special treatment is imposed on one Argo float (2901888; three profiles; Table 1), where the coarse profiles lose data in the upper 20 m; thus, the missing data are filled with the same value as uppermost available data in the near surface.

The data are then projected into the standard CR section (y-coordinate), and the corresponding grid interval is 50 km. ~~with a uniform 100 km interval in the y-coordinate.~~ We use the objective analysis method to interpolate data from irregularly spaced locations to a fixed grid (Barnes, 1994). Later, a low-pass filter is imposed on the CR sectional data to remove the short-wavelength signals, which are partly from the cross-bias among different data sources and partly from the submesoscale or higher wavenumber signals in the real ocean. The low-pass filter is a two-dimensional LOcally Estimated Scatterplot Smoothing (LOESS) filter (Cleveland and Grosse, 1991), and the moving-average wavelengths are 300 km and 30 m in the horizontal and vertical directions, respectively. As a result, the smoothed data save the essential features of the thermal-salinity field but remove the noise.

2.3 Satellite data description

2.3.1 Surface wind

We use Cross-Calibrated Multi-Platform (CCMP; Atlas et al., 2011) gridded surface vector winds here (version 2.0). CCMP data are daily products, and they are projected on 0.25°×0.25° grids.

2.3.2 Sea surface temperature

The sea surface temperature (SST) data is produced by Operational Sea Surface Temperature and Sea Ice Analysis (OSTIA; Donlon et al., 2011), which merges satellite infrared and microwave products, ship, buoy, etc. OSTIA is daily product, and the horizontal resolutions are 0.05$^{\mathrm{o}}\times$0.05$^{\mathrm{o}}$.

2.3.3 Sea surface height

For describing the sea surface height (SSH) and the related surface geostrophic current, we use the Archiving, Validation, and Interpretation of Satellite Oceanographic (AVISO) grided data. The temporal resolution is daily, and the horizontal resolutions are 0.25$^{\mathrm{o}}\times$0.25$^{\mathrm{o}}$.

2.4 Reanalysis data description

As references, we also employ two widely used reanalysis datasets for comparison, aiming at evaluating the quality of reanalysis data. The first reanalysis dataset is Simple Ocean Data Assimilation (SODA, version 3.3.1; Carton and Giese, 2008; Carton et al., 2018), whose horizontal resolutions are 0.25$^{\mathrm{o}}\times$0.25$^{\mathrm{o}}$ for longitude and latitude. The second reanalysis dataset is HYbrid Coordinate Ocean Model (HYCOM, version GOPS3.0:HYCOM+NCODA global 1/12$^{\mathrm{o}}$ Reanalysis GLBu0.08/expt_19.1), and its horizontal resolutions are 0.08$^{\mathrm{o}}\times$0.08$^{\mathrm{o}}$. Both SODA and HYCOM assimilate various in situ and satellite-based data sources: historical station profiles, Argo profiles, moorings, drifters, satellite SSTs, SSHs, etc. For comparison, we extract the reanalysis datasets along the same section as the observations ~~observation~~, and the monthly mean fields are used.

2.5 Method of tracers

Using SODA reanalysis, we release some passive tracers along the CR and backtrack their trajectories based on the Lagrangian description, and the methods are formulated by

$$\begin{cases} X^{n-1/2} & = X^{n+1/2} - U^n \cdot \Delta t \\ Y^{n-1/2} & = Y^{n+1/2} - V^n \cdot \Delta t \\ z^{n-1/2} & = z^{n+1/2} - w^n \cdot \Delta t \end{cases} \tag{1}$$

Here, X and Y are the Cartesian coordinates along longitude and latitude respectively, U and V are the corresponding currents, z is the vertical coordinate, w is the vertical velocity, and n is the time step. In the computation, we use the three dimensional velocity (U, V, w) to track the tracers, and we set the ~~interval of~~ time step (Δt) as 3600 s. The tracers are set along the CR on May 15, 2012, and then backward integrated to January 1, 2010.

3 Results

3.1 Background environment

The time period of the shipboard survey starts ~~start~~ from 2012/05/06 and ends ~~end~~ at 2012/06/01 (Table 1). Figure 2(a-c) show the monthly mean surface wind, SST and SSH, respectively. In this specific month, ~~which is preferentially defined as the later stage of monsoon transition,~~ the summer monsoon has started but is not very strong (Fig. 2a) . The along-coast wind prevails in the regional wind field, and the wind speed in the region far from the western coast is weaker. Positive wind curl along the Somalia coast and Yemen ~~is responsible for off-coast Ekman water transport, which~~ induces sufficient coastal upwelling, which brings ~~to bring~~ lower-layer cold water upward and cools ~~cool~~ the sea surface (Fig. 2b). The patterns of wind curl are roughly consistent with that of the climatological monthly mean wind stress curl (Beal et al., 2013). Otherwise, the ~~dominant~~ wind curl in the NWIO is negative, which is consistent with the annual mean, and forces downwelling ~~denote the downwelling-preferred wind-forcing circumstance~~. The basin-scale semicircular SST contour (30°C) ~~front~~ then outlines a warm area in the oceanic interior~~, where SST exceeds 30°C~~. The main part of the CR is located in this strikingly warm region (Fig. 2b).

On the other hand, SSH (or absolute dynamic height, ADT) shows multiple meso-scale eddies (Fig. 2c). There are some warm-core eddies (anti-cyclonic eddies), to the east of the CR (WCE1), east of the Horn of Africa (WCE2), and northeast of the Horn of Africa but very close to Yemen (WCE3). Two cold-core eddies (cyclonic eddies; CCE1 and CCE2) are also observed at either end of the CR. Besides, a remarkable westward current is observed at the latitude of 6°N, which is noted here as a WPPW ~~westward-propagating disturbance (WPD)~~. WPPW~~WPD~~ is pronounced compared with the circumstances around the specific region, which refers to the zonal extent (7.5° in longitude), while the meridional extent is relatively narrow (1.3° in latitude). The magnitude of zonal current is -0.38 m/s. ~~which refers to not only the magnitude (-0.38 m/s for the zonal current) but also the zonal extent (7.5° in longitude), although its meridional extent is relatively narrow (1.3° in latitude).~~ Furthermore, we investigated the longitude-time plot of the surface zonal current at 6°N latitude (surface geostrophic current from SSH; results are not shown here), the WPPW~~WPD~~ is observed to start at 69°E on day 102, the surface current propagates westward with a phase speed of 0.2 m s^{-1} and arrives at 60°E on day 155.

3.2 Temperature, salinity and density

First, we impose the water mass analysis on the objective-analysis data (section 2.2), and the results are shown in Fig. 3. The data support that the upper water is more saline than the Indian Equatorial Water (IEW) and fresher than the Arabian Sea Water (ASW). The observed waters are likely to be mixed IEW and ASW. When the latitude spans from the equatorial band (2.3-5°N in the present study) to the tropical band (5-9.7°N in the present study), the salinity generally increases, consistent with the northern-side ASW being much more saline than the southern-side IEW (Han et al., 2014) and this meridional variation in salinity is due to the different proportions of IEW and ASW. On the northwest side, water columns contain ASHSW, which are observed as saline water at a potential density of approximately 24 kg/m^3 (Kumar and Prasad, 1999).

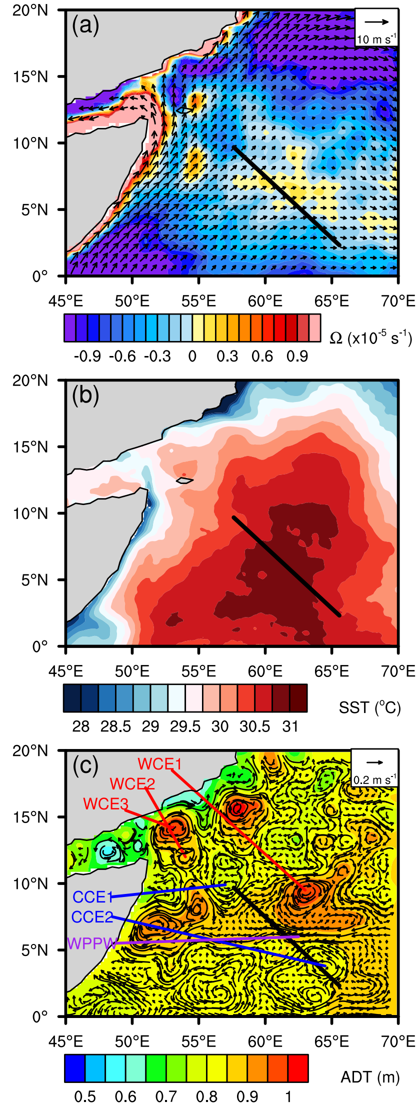

Figure 2. (a) Monthly mean wind vector and vorticity (Ω) from CCMP wind data, data are plotted every 3 points for wind vector; (b) monthly mean sea surface temperature from OSTIA data; and (c) monthly mean sea surface height (absolute dynamic topography), and the consistent surface geostrophic current (shown with every 2 points) from AVISO.

The intermediate waters from our data are projected as PGW (Prasad et al., 2001) and RSW (Beal et al., 2000; Talley et al., 2011). According to Kumar and Prasad (1999), the definition of PGW (RSW) is the density range as 26.2-26.8 kg/m^3 (27.0-27.4 kg/m^3), temperature range 13-19°C (9-11°C), and the salinity range 35.1-37.9 psu (35.1-35.7 psu).

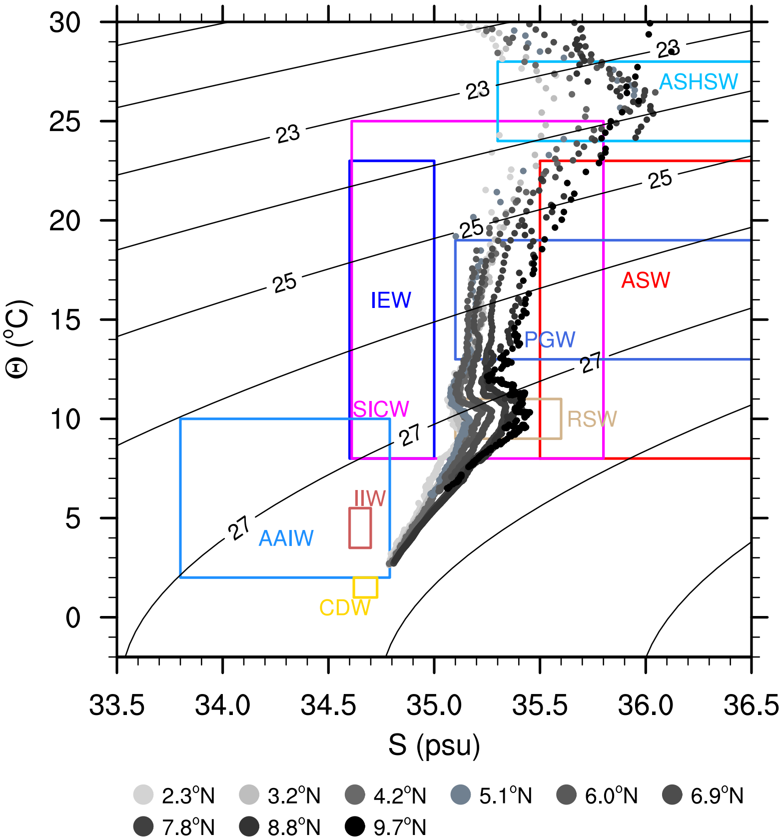

Figure 3. T-S diagram for the upper 2000 m of water on the CR. The water masses are defined in Emery (2001) and include the Arabian Sea water (ASW), Indian equatorial water (IEW), South Indian central water (SICW), Antarctic intermediate water (AAIW), Indonesian intermediate water (IIW), and circumpolar deep water (CDW). The rectangles represent the appropriate temperature and salinity ranges (Table 1 in Emery (2001)). Besides, Red Sea water (RSW), Persian Gulf water (PGW), and Arabian Sea High-Salinity Water (ASHSW) are also represented according to Kumar and Prasad (1999).

Sectional profiles of temperature and salinity are shown in Fig. 4. The thermocline is in the depth range of 100 to 150 m (20°C isothermal line, Xie et al., 2002). From the present observation, the thermocline is nearly flat at the equatorial band and deepens northward in the tropical band. This phenomenon is also supported by the climatological data, which reveal that the sectional distribution of the thermocline is similar to a long-standing geostrophic balanced signal. In the near surface, the isothermal line of 30°C rises ~~some isothermal lines rise~~ to the surface on the northern side and show a clear ventilation structure such that subsurface water can take part in the air-sea interaction. Meanwhile, for the intermediate water, the isothermal line tilts deeper from south to north.

The striking feature of the salinity field is that a salinity tongue appears at 100 m depth, where the salty water is ASHSW (Kumar and Prasad, 1999). Climatological data show that these salty waters originate from the north side and extend southward; however, in our survey, the extent is greater. We emphasize the iso-salinity line of 35.8 psu; the southern extent ~~extension~~ can reach y=150 km (or 6.9°N) in climatology but -250 km (or 4.4°N) in our survey. This result means that the salty water extends southward more than 2.5° in latitude in excess of climatology. The present observation also shows the salty intermediate water as PGW and RSW (Fig. 3). The observation shows slightly more saline water than climatology on the northern side, although the overall structure is mostly consistent with the climatology. In other words, the comparison implies that the year 2002 is an anomaly year for the distributions ~~on the activities~~ of ASHSW, PGW and RSW.

When we move forward to the potential density field, the appearance of the 22 kg/m^3 isopycnal is evident in both the snapshot and climatology. For the snapshot, the outcrop point of the 22 kg/m^3 isopycnal is y=300 km, or 7.8°N. It is worth noting that the outcrop point is near the transition point for signs of wind vorticity (Fig. 2a), and the results suggest that the ventilation is induced by surface wind. The north side of the outcrop point has negative wind vorticity, which promotes downwelling. Ventilation is highly related to the downwelling of high-salinity water and its southern extent ~~extension~~ (Luyten et al., 1983).

Fig. 4 also shows the reanalysis data, and essentially, the reanalysis captures the thermal structure quite well compared with the present observations and climatology. For instance, in the upper ocean, the surface warm water is distributed on the south side and northward to y=400 km where the isothermal line of 30°C ~~it~~ crops out. The observed ~~steeply~~ descending thermocline near y=100 km is recognizable ~~reproduced~~ in SODA and HYCOM. It is also noted that the equatorial near-surface upwelling in HYCOM has some evidence from the present observations. For the intermediate-depth water, in SODA and HYCOM, the isothermal lines also tilt deeper from south to north, which resembles both the present observations and the climatology.

For salinity, the southward extent ~~extension~~ of ASHSW is also captured by SODA and HYCOM, and the southward extent ~~extension~~ in HYCOM approaches the observations more closely. In the intermediate-depth water, the southward extent ~~extension~~ from the north side in SODA is similar to the observations, while the corresponding signal in HYCOM is obscured.

The upper ocean density fields from SODA and HYCOM also show clear ventilation structures. From the observations, equatorial waters with a potential density of 22 kg/m^3 at a depth of 30 m are rising to the surface. The outcrop points of potential density of 22 kg/m^3 in SODA and HYCOM are shifted southward compared with the observations. Additionally, the near-surface upwelling in the equatorial band in HYCOM is strong, but not significant in the observations.

3.3 Cross-track current

The geostrophic current is deduced from the in situ density field by thermal wind theory (Fig. 5), where the velocity is integrated downward from the surface geostrophic current (Lagerloef et al., 1999). The velocity field is relatively strong in the upper ocean, where the current field is dominated by meso-scale eddies. The cross-track current in the equatorial band is induced by CCE2. The structure of CCE2 is asymmetric, and the positive cross-track flow is stronger than the negative counterpart. In contrast, the northwest side of CR is identified as the south part of CCE1 (northeastward flow). At 6°N latitude, the vertical structure of WPPW~~WPD~~ is well rebuilt in Fig. 5a. WPPW~~WPD~~ seems to extend vertically to a depth of 200 m, and the horizontal extent is near 200 km for the current greater than 0.02 m/s. Meanwhile, the maximum cross-track current of the WPPW ~~disturbance~~ is 0.12 m/s. ~~Furthermore, we investigated the surface zonal current at 6°N latitude (surface geostrophic current from SSH), the WPPWWPD is are observed to start at 69°E on day 102, the surface current propagates propagate westward with a phase speed of 0.2 m s^{-1} and arrives arrive at 60°E on day 155 (results are not shown here).~~ The current field also captures the northeastward current (less than 0.075 m/s) in the intermediate depth (-200 $\leq y \leq$ -20 km, and 150 $\leq y \leq$ 350 km), which is due to the corresponding isothermal tilting (Fig. 4).

For the reanalysis data, as shown in Fig. 5, although the surface currents are similar due to the assimilation of SSH in the reanalysis process, the cross-track current from reanalysis is quite different from the observation-based absolute geostrophic current. The differences are observed in three aspects. First, the meso-scale eddy CCE2 is not well represented for the vertical structure, as SODA and HYCOM limit the southern part of CCE2 to the upper 200 m, when the current speed is faster than 0.05 m/s. Meanwhile, in SODA and HYCOM, the northern part of the meso-scale eddy (CCE2) has much latitude expansion, and merges the WPPW ~~disturbance (WPD)~~. Second, the undercurrent in the southern portion of the observations differs from those in SODA and HYCOM. The undercurrent in SODA is relatively weak, while HYCOM shows a northward shift of the current core. Finally, for the northern portion, SODA gives a relatively shallow depth for the surface northeastward current, and the corresponding horizontal extent exceeds that of the observations. The locations of surface zero current in SODA and observation are y=170 and 240 km, respectively.

Part of the difference between observation-based absolute geostrophic current and reanalysis current is due to the near-surface Ekman current. The mean surface Ekman speed, which is approximately the difference between surface geostrophic current and in-situ surface current (from surface drifter), is within 0.1 m/s in northern IO (Saj, 2017). Besides, the climatological monthly mean mixed-layer depth in May is roughly 20 m at station 9.5°N and 59.5°E (on CR; Liu et al., 2018). ~~The climatological monthly mean mixed-layer depth in May is roughly 20 m at station 9.5°N and 59.5°E (on CR; Liu et al.,, 2018). Besides, the mean surface Ekman speed, which is approximately the difference between surface geostrophic current and in-situ surface current (from surface drifter), is within 0.1 m/s in northern IO (Saj, 2017).~~ Considering the near-surface Ekman current decays exponentially with depth, therefore ~~Therefore~~, the near-surface Ekman currents in reanalysis datasets are relatively weak to affect the main results as mentioned above.

3.4 Tracers

Here, the SODA reanalysis supplies compact datasets for passive tracers; therefore, we set some passive tracers along the CR and backtrack their trajectories using the Lagrangian description (section 2.5), and the results are shown in Fig. 6. For the ASHSW, we set the tracers at a depth of 100 m, and the trajectories reveal different pathways on the CR. For better describing the trajectories, we separate the CR to three latitude bands as 2.3-5°N (equatorial band), 5-8°N and 8-9.8°N. In the equatorial band (Fig. 6e), the near-equator tracers come from the west side, which is consistent with the north branch of East African Coastal Current during summer monsoon (Schott and McCreary Jr., 2001; Schott et al., 2009). Meanwhile, for the relatively north-side tracers in equatorial band, the trajectories backtrack to east side, which is probably following a westward current or meso-scale eddy. While for latitudes from 5-8°N (Fig. 6c), the water mainly originates from the northeast side, and the trajectories resemble those of the ventilation theory (Luyten et al., 1983; Qiu and Huang, 1995). The results support ASHSWs are mainly from the Arabian Basin, ~~which agrees with the ASHSW definition,~~ and the southwestward flow bring the ASHSW into CR. In some occasions, the 100 m depth waters in this latitude section are from the equator, and the pathways show the north branch of East African Coastal Current and the cross-equatorial current around 66°E respectively. Similarly, the pathways start at the east of the Horn of Africa are probably due to the off-coast current at the north of Great Whirl or meso-scale eddies (Chelton et al., 2011; Wang et al., 2019). For latitudes from 8-9.8°N (Fig. 6a), the trajectories emphasis the north branch of East African Coastal Current, meanwhile, the water at the north station of CR comes from the northeast side, and one station water shows the cross-equatorial current around 53°E (east of Southern Gyre; Schott et al., 2009).

For the RSW in the intermediate-depth layer at 700 m, the trajectories in the equatorial band (Fig. 6f) show the zonal movement. Most of the trajectories move from the west side, which coincident with the potential vorticity explanation (Beal et al., 2000), that the RSW moves southward along the coast with the help of winter monsoon, and then leave the coast and shift to middle ocean via zonal movement. Other two trajectories come from east side, and one extra trajectory moves from northwest with circular track. Hence, these trajectories display three kinds of pathways. Accordingly, in the 5-8°N band (Fig. 6d), the mainly eastward zonal movements agree with Beal et al. (2000), meanwhile, some westward trajectories resemble the ventilation theory (Luyten et al., 1983; Qiu and Huang, 1995). At last, in the 8-9.8°N (Fig. 6b), new pathway directly from northwest is emerged, and the trajectories support 700 m waters are probably directly from east of the Horn of Africa (or Gulf of Aden) without southward movements along the coast.

4 Discussion

The CTD and XCTD data are precise in reconstructing the three-dimensional oceanic data. Based on theoretical model, three-dimensional ocean interior can be derived using surface information (SSH and sea surface density), where the reliable mean density field is required (Lapeyre and Klein, 2006; Wang et al., 2013; Liu et al., 2014; Yan et al., 2020). In other words, for the operational purpose, the meso-scale eddy coherent structure could be built on known background density field. The Argo-only data are not sufficient to describe the meso-scale eddy in the NWIO, thus could not supply sufficient background density. In the present study, the maximum distance between Argo profiles is 500 km along the CR; however, after adding the shipboard station data, the maximum distance decreases to 100 km, which falls into the eddy-permitting scale. Sufficient sampling produces more reliable vertical structures of temperature, salinity and density.

The most remarkable signal in the upper ocean is the southward extent ~~extension~~ of ASHSW, where the counterpart in the climatology data exists but is weak in the horizontal extent ~~extension~~. It is surprising that the HYCOM reanalysis captures the phenomenon well, while SODA shows some disadvantages. Although both SODA and HYCOM assimilate the Argo data into Oceainc General Circulation Models (OGCMs), the assimilation methods of SODA and HYCOM are considerably different. SODA adopts optimal interpolation (Carton et al., 2018), while HYCOM uses a 3D varational ~~3D variation~~ scheme. One advantage of a 3D variational ~~3D variation~~ scheme versus optimal ~~optimum~~ interpolation is the conservation of dynamical constraints ~~constrains~~ (Zhu et al., 2006; Yin et al., 2012; Edwards et al., 2015). Therefore, HYCOM probably describes better ~~on~~ the wind-driven circulations, monsoon-induced coastal current and meso-scale eddy movement, which are all related to the southward extent ~~extension~~ of ASHSW. In the comparative analysis, the state-of-the-art reanalysis is still insufficient to provide good current data. Although similar sea surface dynamic heights are taken into account, the incorrect density field leads to a false vertical structure ~~mode~~. It is also noted that the bias is probably further amplified in OGCM and leads to potential unrealistic simulations if these reanalysis data are used in the model for initialization and boundary forcing.

From the theoretical viewpoint, the phase speed of first-, second- and third-mode baroclinic Rossby wave at 6°N in Indian Ocean is roughly 0.6, 0.2 and 0.1 m/s, respectively (Subrahmanyam et al., 2001). The phase speed of WPPW match well with that of the second-mode baroclinic Rossby wave. For the generation mechanics, Subrahmanyam et al. (2001) argued that this kind Rossby wave was probably radiated from coastal trapped Kelvin wave at south-west coast of Indian. Meanwhile, this kind Rossby wave can bring wave energy from south-west coast of Indian to the Somali coast, and feed the Somali Current and Somali eddies. The present study displays the vertical structure of this kind Rossby wave, however, the dynamics of WPPW (and Rossby wave) and the its association with Somali Current and Somali eddies call for further study.

Generally, the hydrothermal plume in CR uplifts from sea bottom to water depth 2500 m (Murton et al., 2006; Wang et al., 2017). Present paper restricts the sectional study to ~~in~~ the upper 1050 m (Fig. 4-5). Within this depth, the water is easily ~~easy~~ affected by surface forcing. However, on the basin-scale wind-driven circulation, the surface wind forcing affects deeper ocean through quasi-geostrophic instability (Rhines and Young, 1982) and meridional overturning circulation. ~~Generally, the hydrothermal plume in CR uplifts from sea bottom to water depth 2500 m (Murton et al., 2006; Wang et al., 2017).~~ Because present paper concentrates on the CR as well as the cross-ridge current, the upper 1050 m dynamics towards the upper ocean cross-ridge water transport, which is related to the deeper ocean dynamics through pressure adjustment, meanwhile, the activity of meso-scale eddy induces deeper ocean vorticity response (Rhines and Young, 1982), the results provide potential use in the future study of hydrothermal plume event.

5 Conclusions

This paper reports a onetime hydrographic survey on the CR in the NWIO, where the latitudes cover the equatorial (2.3-5°N) and tropical (5-9.6°N) bands. The station CTD/XCTD sampling plus the Argo floats build the sectional structures of temperature and salinity as well as density. The striking feature is the southern extent ~~extension~~ of ASHSW from northwest of the CR in the upper ocean. Meanwhile, the temperature and density fields display clear ventilation structures. In the intermediate depth, the observations also capture the RSW at a depth near 700 m.

Furthermore, we compute the absolute geostrophic current based on the density profiles and sea surface height. The vertical structure of the cross-track current reveals strong signals of meso-scale eddies in the upper ocean and relatively weak north-eastward current in the intermediate depth. We also identify a strong westward-propagating planetary wave ~~disturbance~~ at a latitude of 6°N. The longitude and latitude lengths are 7.5° and 1.3° respectively. The corresponding phase speed is 0.2 m/s, and the vertically affected depth is roughly 200 m.

We further evaluate the state-of-the-art reanalysis with the present observations. As a result, because the Argo profiles and satellite SSH are assimilated into the reanalysis datasets, HYCOM and SODA show relatively good qualities for temperature, salinity and density. However, the reanalysis cross-track currents show large discrepancies compared with the absolute geostrophic current. Most importantly, HYCOM and SODA misinterpret some meso-scale eddies in the current field. Over the NWIO, the meso-scale eddies are relatively important but cannot be well described by the Argo-only data source. The present analysis shows more data source for potential data assimilation experiment. The present situation of insufficient sampling prompts more research activity in the NWIO.

To explore the pathways of ASHSW and RSW during the expedition time, we set tracers in SODA dataset at depths of 100 and 700 m, and backtrack their trajectories via three dimensional Lagrangian description. Overall, for the 100 m depth waters, the results reveal the pathways related to the north branch of East African Coastal Current and the flow from northeast side (or Arabian Basin), while for the 700 m depth waters, the trajectories mainly follow the zonal direction from either west and east sides. The results give direct-viewing descriptions and call for further dynamical investigations.

Competing interests. The authors declare that they have no conflict of interest.

Acknowledgements. This work is supported by the China Ocean Mineral Resources Research and Development Association Project (Nos. DY135-S2-1-07 and DY135-E2-1-01) and the National Natural Science Foundation of China (Nos. 41730535 and 41621064). OSTIA SST data were produced by the Meteorological Office of the United Kingdom (http://marine.copernicus.eu/). We are thankful to editor and two anonymous reviewers for their constructive suggestions and comments. WOA data were available in https://www.nodc.noaa.gov/. Daily Argo float data were downloaded from http://www.argodatamgt.org. CCMP wind were provided by Remote Sensing Systems (http://www.remss.com, version 2.0), AVISO SSH data were produced and distributed by the Copernicus Marine and Environment Monitoring Service (CMEMS) (http://www.marine.copernicus.eu), SODA were obtained from http://www.atmos.umd.edu/ ocean/, and HYCOM were downloaded from https://hycom.org/.

References

Atlas, R., Hoffman, R. N., Ardizzone, J., Leidner, S. M., Jusem, J. C., Smith, D. K., and Gombos, D.: A cross-calibrated, multiplatform ocean surface wind velocity product for meteorological and oceanographic applications, Bull. Amer. Meteor. Soc., 92, 157–174, 2011.

Barnes, S. L.: Applications of the Barnes Objective Analysis Scheme. Part I: Effects of Undersampling, Wave Position, and Station Randomness, J. Atmos. Oceanic Technol., 11, 1433–1448, 1994.

Beal, L. M., Ffield, A., and Gordon, A. L.: Spreading of Rea Sea overflow waters in the Indian Ocean, J. Geophys. Res., 105, 8549–8564, 2000.

Beal, L. M., Hormann, V., Lumpkin, R., and Foltz, G.: The Response of the Surface Circulation of the Arabian Sea to Monsoonal Forcing, J. Phys. Oceanogr., 43, 2008–2022, 2013.

Carton, J. A. and Giese, B. S.: A reanalysis of ocean climate using Simple Ocean Data Assimilation (SODA), Monthly Weather Review, 136, 2999–3017, 2008.

Carton, J. A., Chepurin, G. A., and Chen, L. G.: SODA3: A new ocean climate reanalysis, J. Clim., 31, 6967–6983, 2018.

Chelton, D. B. and Schlax, M. G.: Global observations of oceanic Rossby waves, Science, 272, 234–238, 1996.

Chelton, D. B., Schlax, M. G., and M., S. R.: Global observations of nonlinear mesoscale eddies, Progress in Oceanography, 91, 167–216, 2011.

Chen, G. X., Han, W. Q., Li, Y. L., Wang, D. X., and J., M. M.: Seasonal-to-interannual time scale dynamics of the equatorial undercurrent in the Indian Ocean, J. Phys. Oceanogr., 54, 1532–1553, 2015.

Cleveland, W. S. and Grosse, E.: Computational methods for local regression, Stat. Comput., 1, 47–62, 1991.

Donlon, C. J., Martin, M., Stark, J. D., Roberts-Jones, J., E., F., and W., W.: The Operational Sea Surface Temperature and Sea Ice analysis (OSTIA), Remote Sensing of the Environment, 116, 140–158, 2011.

Edwards, C. A., Moore, A. M., Hoteit, I., and Cornuelle, B. D.: Regional ocean data assimilation, Annual Review of Marine Science, 7, 21–42, 2015.

Emery, W. J.: Water Types and Water Masses*, in: Encyclopedia of Ocean Sciences (Second Edition), edited by Steele, J. H., pp. 291 – 299, Academic Press, Oxford, second edition edn., https://doi.org/https://doi.org/10.1016/B978-012374473-9.00108-9, 2001.

Han, W. Q., Vialard, J., McPhaden, M. J., Lee, T., Masumoto, Y., Feng, M., and DE Ruijter, W. P. M.: Indian Ocean decadal variability: A review, Bulletin of the American Meteorological Society, 95, 1679–1703, 2014.

Kumar, S. P. and Prasad, T. G.: Formation and spreading of Arabian Sea high-salinity water mass, J. Geophys. Res. Oceans, 104, 1455–1464, 1999.

Lagerloef, G. S. E., Mitchum, G. T., Lukas, R. B., and Niiler, P. P.: Tropical Pacific near-surface currents estimated from altimeter, wind, and drifter data, J. Geophys. Res.-Oceans, 104, 23 313–23 326, 1999.

Lapeyre, G. and Klein, P.: Dynamics of the Upper Oceanic Layers in Terms of Surface Quasigeostrophy Theory, Journal of Physical Oceanography, 36, 165–176, https://doi.org/10.1175/JPO2840.1, 2006.

Li, Y. L. and Han, W. Q.: Decadal sea level variations in the Indian Ocean investigated with HYCOM: Roles of climate modes, ocean internal variability, and stochastic wind forcing, J. Clim., 28, 9143–9165, 2015.

Liu, L., Peng, S., Wang, J., and Huang, R. X.: Retrieving density and velocity fields of the ocean's interior from surface data, Journal of Geophysical Research: Oceans, 119, 8512–8529, https://doi.org/10.1002/2014JC010221, 2014.

Liu, L. L., Huang, R. X., and Wang, F.: Ventilation of a monsoon-dominated ocean: Subduction and obduction in the North Indian Ocean, J. Geophys. Res. Oceans, 123, 4449–4463, 2018.

Luyten, J. L., Pedlosky, J., and Stommel, H. M.: The ventilated thermocline, J. Phys. Oceanogr., 13, 292–309, 1983.

McCreary, J. P.: Modeling equatorial ocean circulation, Annual Review of Fluid Mechanics, 17, 359–409, 1985.

Murton, B. J., Baker, W. T., Sands, C. M., and German, C. R.: Detection of an unusually large hydrothermal event plume above the slow-spreading Carlsberg Ridge: NW Indian Ocean, Geophys. Res. Lett., 33, L10608, 2006.

Prasad, T. G., Ikeda, M., and Kumar, S. P.: Seasonal spreading of the Persian Gulf Water mass in the Arabian Sea, J. Geophys. Res. Oceans, 106, 17 059–17 071, 2001.

Qiu, B. and Huang, R. X.: Ventilation of the North Atlantic and North Pacific: Subduction versus obduction, J. Phys. Oceanogr., 25, 2374–2390, 1995.

Rhines, P. B.: Waves and turbulence on a beta-plane, J. Fluid Mech., 69, 417–443, 1975.

Rhines, P. B. and Young, W. R.: Homogenization of potential vorticity in planetary gyres, J. Fluid Mech., 122, 347–367, 1982.

Riser, S. C., Freeland, H. J., Roemmich, D., Wijffels, S., Troisi, A., Belbeoch, M., Gilbert, D., Xu, J., Pouliquen, S., Thresher, A., Le Traon, P.-Y., Maze, G., Klein, B., Ravichandran, M., Grant, F., Poulain, P.-M., Suga, T., Lim, B., Sterl, A., Sutton, P., Mork, K.-A., Velez-Belchi, P. J., Ansorge, I., King, B., Turton, J., Baringer, M., and Jayne, S. R.: Fifteen years of ocean observations with the global Argo array, Nature Climate Change, 6, 145–153, 2016.

Saj, R. P.: Surface velocity estimates of the North Indian Ocean from satellite gravity and altimeter missions, International Journal of Remote Sensing, 38, 296–313, 2017.

Saji, N. H., Goswami, B. N., Vinayachandran, P. N., and Yamagata, T.: A dipole mode in the tropical Indian Ocean, Nature, 401, 360–363, 1999.

Schott, F. A. and McCreary Jr., J. P.: The monsoon circulation of the Indian Ocean, Progress in Oceanography, 51, 1–123, 2001.

Schott, F. A., Xie, S. P., and McCreary Jr., J. P.: Indian Ocean circulation and climate variability, Reviews of Geophysics, 47, RG1002, 2009.

Sharma, G. S., Gouveia, A. D., and Satyendranath, S.: Incursion of the Pacific Ocean water into the Indian Ocean, Proc. Indian Acad. Sci., 87A, 29–45, 1978.

Subrahmanyam, B., Robinson, I. S., Blundell, J. R., and Challenor, P. G.: Indian ocean Rossby waves observed in TOPEX/POSEIDON altimeter data and in model simulations, International Journal of Remote Sensing, pp. 141–167, 2001.

Talley, L. D., Pickard, G. L., Emery, W. J., and S., J. H.: Descriptive physical oceanography: An introduction, Elsevier, Burlingham, 6 edn., 2011.

Vecchi, G. A., Xie, S. P., and Fischer, A. S.: Ocean-atmosphere covariability in the Western Arabian Sea, Journal of Climate, 17, 1213–1224, 2004.

Vitale, S. S., DiMarco, S. F., Seidel, H. F., and Wang, Z. K.: Circulation analysis in the northwest Indian Ocean using ARGO floats and surface drifter observations, and SODA reanalysis output, Dynamics of Atmospheres and Oceans, 78, 57–70, 2017.

Wang, J., Flierl, G. R., LaCasce, J. H., McClean, J. L., and Mahadevan, A.: Reconstructing the Ocean's Interior from Surface Data, Journal of Physical Oceanography, 43, 1611–1626, https://doi.org/10.1175/JPO-D-12-0204.1, 2013.

Wang, S., Zhu, W. J., Ma, J., Ji, J. L., Yang, J. S., and Dong, C. M.: Variability of the Great Whirl and its impacts on atmospheric processes, Remote Sensing, 11, 322, 2019.

Wang, Y. J., Han, X. Q., Petersen, S., Frische, M., Qiu, Z. Y., Li, H. M., Li, H. L., Wu, Z. C., and Cui, R. Y.: Mineralogy and trace element geochemistry of sulfide minerals from the Wocan Hydrothermal Field on the slow-spreading Carlsberg Ridge Indian Ocean, Ore Geology Reviews, 84, 1–19, 2017.

Webster, P. J., Moore, A. M., Loschnigg, J. P., and Leben, R. R.: Coupled ocean-atmosphere dynamics in the Indian Ocean during 1997-98, Nature, 401, 356–360, 1999.

Xie, S. P., Annamalai, H., Schott, F. A., and McCreary Jr., J. P.: Structure and mechanisms of south Indian Ocean climate variability, J Clim, 15, 864–878, 2002.

Yan, H., Wang, H., Zhang, R., Chen, J., Bao, S., and Wang, G.: A Dynamical-Statistical Approach to Retrieve the Ocean Interior Structure From Surface Data: SQG-mEOF-R, Journal of Geophysical Research: Oceans, 125, e2019JC015 840, https://doi.org/10.1029/2019JC015840, 2020.

Yang, G., He, H. L., Wang, Y., Han, X. Q., and Wang, Y. J.: Evaluating a satellite-based sea surface temperature by shipboard survey in the Northwest Indian Ocean, Acta Oceanologica Sinica, 35, 52–58, 2016.

Yin, X. Q., Qiao, F. L., Yang, Y. Z., Xia, C. S., and Chen, X. Y.: Argo data assimilation in ocean general circulation model of Northwest Pacific Ocean, Ocean Dynamics, 62, 1059–1071, 2012.

You, Y.: Intermediate water circulation and ventilation of the Indian Ocean derived from water-mass contributions, Journal of Marine Research, 56, 1029–1067, https://doi.org/doi:10.1357/002224098765173455, 1998.

Zhu, J., Zhou, G. Q., X., Y. C., Fu, W. W., and You, X. B.: A three-dimensional variational ocean data assimilation system: Scheme and preliminary results, Science in China Series D: Earth Sciences, 49, 1212–1222, 2006.

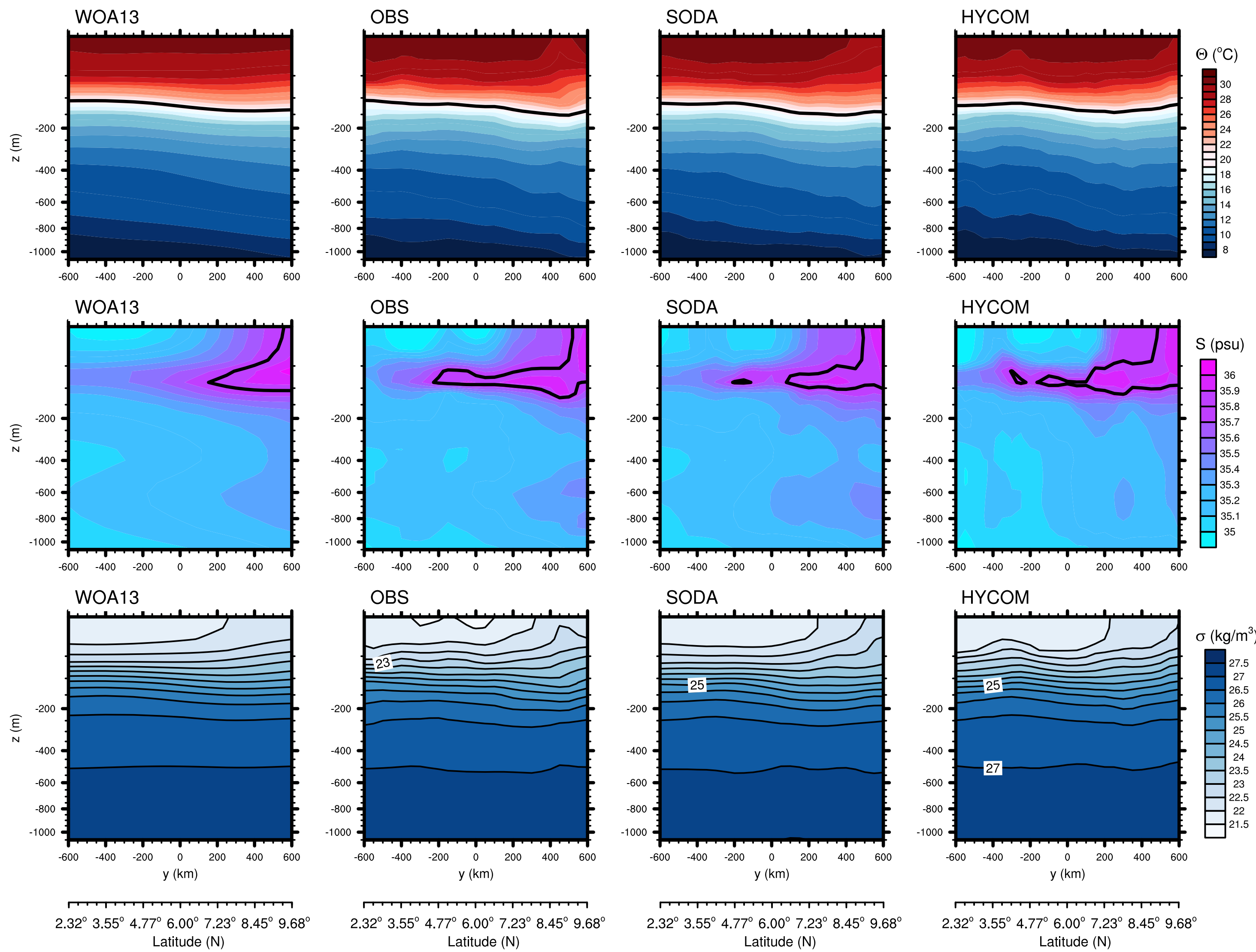

Figure 4. Sectional profiles of potential temperature (upper panels), salinity (middle panels) and potential density (lower panels). The data sources cover the WOA climatology (WOA13, version 2.0/A5B2), the present observations, and two reanalysis datasets, SODA and HYCOM. The isothermal lines of 20°C are ~~presented at~~ highlighted in the potential temperatures, and the iso-salinity lines of 35.8 psu are highlighted in the salinity fields.

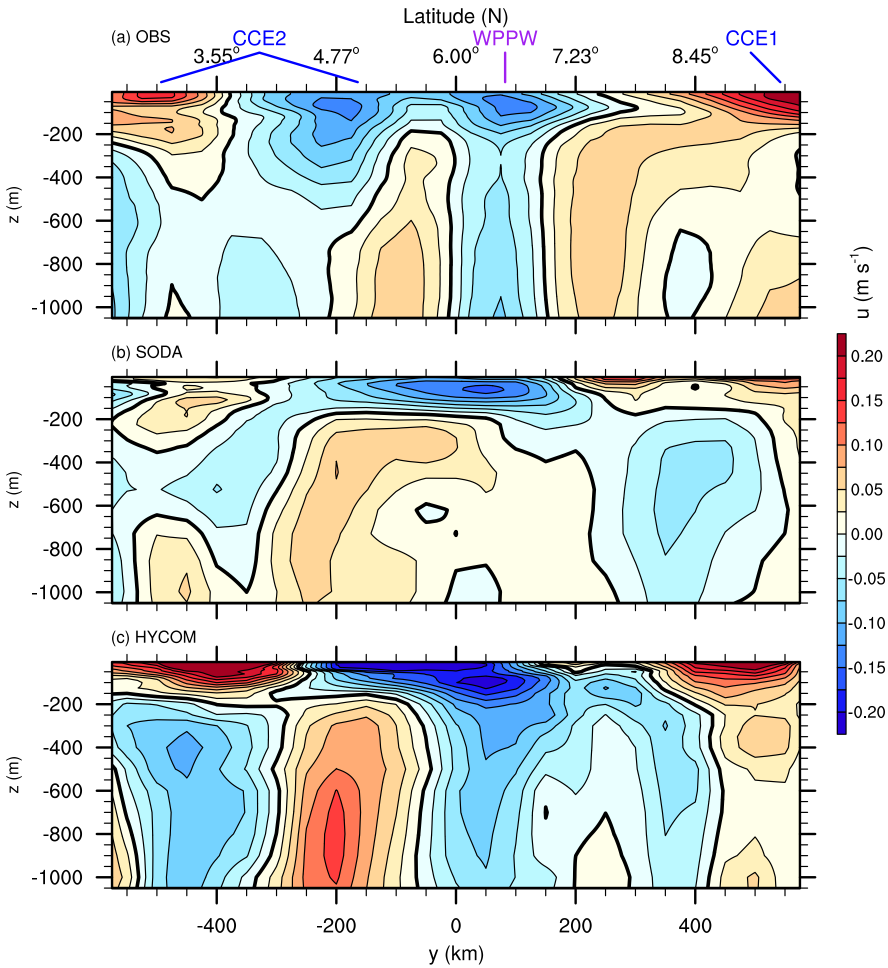

Figure 5. Sectional cross-track current: (a) absolute geostrophic current; (b and c) currents in SODA and HYCOM reanalysis, respectively. Northeastward current is positive. Thick black lines are the zero contours.

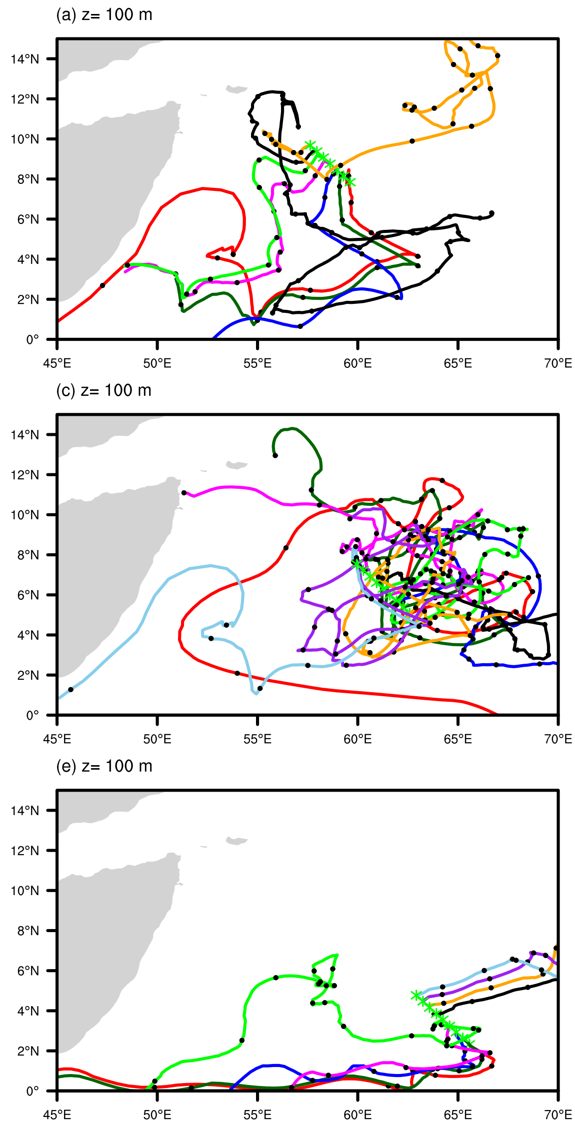

Figure 6. Passive tracers using SODA reanalysis. The time interval is one month, as denoted by the black dots. (a-b) 8-9.8°N; (c-d) 5-8°N; (e-f) 2-5°N.